

# Discrete spatial solitons in a diffraction-managed nonlinear waveguide array: a unified approach

Mark J. Ablowitz\*, Ziad H. Musslimani

*Department of Applied Mathematics, University of Colorado at Boulder, Campus Box 526, Boulder, CO 80309-0526, USA*

---

## Abstract

Localized, stable nonlinear waves, often referred to as solitons, are of broad interest in mathematics and physics. They are found in both continuous and discrete media. In this paper, a unified method is presented which is used to describe the propagation of linearly polarized light as well as two polarization modes in a diffraction-managed nonlinear waveguide array. In the regime of normal diffraction, both stationary and moving discrete solitons are analyzed using the Fourier transform method. The numerical results based on a modified Neumann iteration scheme as well as renormalization techniques, indicate that traveling wave solutions are unlikely to exist. An asymptotic equation is derived from first principles which governs the propagation of electromagnetic waves in a waveguide array in the presence of both normal and anomalous diffraction. This is termed diffraction management. The theory is then extended to the vector case of coupled polarization modes.

© 2003 Elsevier B.V. All rights reserved.

*Keywords:* Nonlinear waves; Discrete spatial soliton; Diffraction

---

## 1. Introduction

Dynamics of discrete nonlinear systems dates back to the mid-fifties when Fermi, Pasta and Ulam (FPU) studied dynamics of nonlinear springs [1]. Apart from the fact that the work of FPU motivated the discovery of solitons, it also stimulated considerable interest in the study of discrete nonlinear media which possesses self-confined structures (discrete solitary waves). Such waves are localized modes of nonlinear lattices that form when “discrete diffraction” is balanced by nonlinearity. In physics a soliton usually denotes a stable localized wave structure, i.e., solitary wave. We shall use the term soliton in this broader sense (i.e., they do not necessarily interact elastically). Discrete solitons have been demonstrated to exist in a wide range of physical systems [2–5]. For example, atomic chains [6,7] (discrete lattices) with an on-site cubic nonlinearities, molecular crystals [8], biophysical systems [9], electrical lattices [10], and recently in arrays of coupled nonlinear optical waveguides [11,12]. An array of coupled optical waveguides is a setting that represents a convenient laboratory for experimental observations.

The first theoretical prediction of discrete solitons in an optical waveguide array was reported by Christodoulides and Joseph [13]. Later, many theoretical studies of discrete solitons in a waveguide array reported switching, steering and other collision properties of these solitons [14–19] (see also the review papers [20,21]). In all the above cases, the

---

\* Corresponding author.

*E-mail address:* [markjab@newton.colorado.edu](mailto:markjab@newton.colorado.edu) (M.J. Ablowitz).

localized modes are solutions of the well known discrete nonlinear Schrödinger (DNLS) equation which describes beam propagation in Kerr nonlinear media (according to coupled mode theory). Discrete bright and dark solitons have also been found in quadratic media [22], in some cases, their properties differ from their Kerr counterparts [23].

In fact, the DNLS equation (and its “cousins” such as diffraction-managed discrete nonlinear Schrödinger (DM-DNLS) or DNLS with a potential such as discrete BEC) is “asymptotically universal”. Namely it is the discrete equation which emerges from either a weakly nonlinear Helmholtz equation with a suitable “potential” or a weakly nonlinear continuous NLS equation with a suitable potential where the following terms are in balance:

- (i) Slow variation in either distance (waveguide array) or time (for BEC);
- (ii) linear terms induced by a potential which can be viewed as asymptotically separated localized potentials (sometimes called the “tight binding approximation”);
- (iii) nonlinearity.

It took almost a decade until self-trapping of light in discrete nonlinear waveguide array was experimentally observed [11,12]. When a low intensity beam is injected into one or a few waveguides, the propagating field spreads over the adjacent waveguides hence experiencing discrete diffraction. However, at sufficiently high power, the beam self-traps to form a localized state (a soliton) in the center waveguides. Subsequently, many interesting properties of nonlinear lattices and discrete solitons were reported. For example, the experimental observation of linear and nonlinear Bloch oscillations in: AlGaAs waveguides [24], polymer waveguides [25] and in an array of curved optical waveguides [26]. Discrete systems have unique properties that are absent in continuous media such as the possibility of producing *anomalous* diffraction [27]. Hence, self-focusing and defocusing processes can be achieved in the same medium (structure) and wavelength. This also leads to the possibility of observing discrete dark solitons in self-focusing Kerr media [28]. The recent experimental observations of discrete solitons [11] and diffraction management [27] have motivated further interests in discrete solitons in nonlinear lattices. This includes the newly proposed model of discrete diffraction-managed nonlinear Schrödinger equation [29,30] whose width and peak amplitude vary periodically, optical spatial solitons in nonlinear photonic crystals [31–33] and the possibility of creating discrete solitons in Bose–Einstein condensation [34]. Also, recently, it was shown that discrete solitons in two-dimensional networks of nonlinear waveguides can be used to realize intelligent functional operations such as blocking, routing, logic functions and time gating [35–38]. In addition, spatiotemporal discrete solitons have been recently suggested in nonlinear chains of coupled microcavities embedded in photonic crystal structures [39].

In this paper, we introduce the Fourier transform method to analyze both stationary and moving solitons in nonlinear lattices. The essence of the method is to transform the DNLS equation governing the solitary wave into Fourier space, where the wave function is smooth, and then deal with a nonlinear nonlocal integral equation for which we employ a rapidly convergent numerical scheme to find solutions. A key advantage of the method is to transform a differential-delay equation into an integral equation for which computational methods are effective. Mathematically, the method also provides a foundation upon which an analytic theory describing solitons in nonlinear lattices can be constructed. We shall consider in this paper two important models: the DNLS equation and the DM-DNLS equation. Applying this method to the first model, shows that approximate traveling solitons possess a nontrivial nonlinear “chirp”. Moreover, our results (both numerical and analytical) indicate that, unlike the integrable case [40], a continuous exact traveling wave (TW) solution is unlikely to exist [41]. In the limit of small velocity, we develop a fully discrete perturbation theory and show that slowly but not uniformly moving discrete solitons are indeed “chirped”. An asymptotic equation is derived from first principles which governs the propagation of electromagnetic waves in a waveguide array in the presence of both normal and anomalous diffraction. This is related to the second model of DM-DNLS equation. The theory is then extended to the vector case of coupled polarization modes.

The new results of this paper can be summarized as follows:

- The derivation of the DNLS equation based on asymptotic multiple scale theory starting, e.g., from the Helmholtz equation.
- The derivation of the scalar DM-DNLS equation from first principles. Using multiple scale asymptotic theory it is found that the most general equation that governs the dynamics of light propagating in a diffraction-managed waveguide array is

$$i \frac{\partial E_n}{\partial z} + \mathcal{C}(z)E_{n+1} + \mathcal{C}^*(z)E_{n-1} + \nu|E_n|^2 E_n = 0,$$

where  $E_n$  is the slowly varying envelope of the electric field at site  $n$ ,  $\nu$  a constant that measures the nonlinear refractive index,  $\mathcal{C}(z)$  a complex periodic function and  $*$  the complex conjugate.

- The derivation from first principles of the vector DM-DNLS equation which includes self and cross-phase modulation as well as four-wave mixing (FWM) terms:

$$i \frac{\partial A_n}{\partial z} + k_{\text{wg}}A_n + \mathcal{C}(z)A_{n+1} + \mathcal{C}^*(z)A_{n-1} + (|A_n|^2 + b_1|B_n|^2)A_n + \eta_1 B_n^2 A_n^* = 0,$$

$$i \frac{\partial B_n}{\partial z} + k_{\text{wg}}B_n + \mathcal{C}(z)B_{n+1} + \mathcal{C}^*(z)B_{n-1} + (|B_n|^2 + b_2|A_n|^2)B_n + \eta_2 A_n^2 B_n^* = 0,$$

where  $A_n$ ,  $B_n$  are the slowly varying envelopes of the two polarization fields at site  $n$ ,  $b$  the cross-phase modulation coefficient and  $\eta$  the strength of FWM term. We note that even the derivation of the constant diffraction case is new.

- A numerical scheme based on renormalization of suitable norms to solve the nonlinear integral equation governing solitons is proposed.
- Based on asymptotic and numerical evidence, we conclude that it is unlikely that a *uniformly* moving TW exists for the DNLS equation.
- The derivation of a new discrete nonlinear Schrödinger type equation.

The paper is organized as follows. In [Section 2](#) we formulate the basic physical model and describe the asymptotic analysis that leads to the DNLS equation. Linear propagation is discussed in both normal and anomalous regimes. In [Section 3](#) we introduce the discrete Fourier transform method to find soliton solutions and show how one can obtain approximate TW solutions. Two numerical schemes are introduced. The first is based on modified Neumann iteration and the second on renormalization. Analytical analysis of TWs based on asymptotic theory is provided in [Section 4](#) which further support our conjecture that *exact* TWs may not exist. Next, we set up in [Section 5](#) a physical model that describes the propagation of two interacting optical fields in a nonlinear waveguide array with varying diffraction. Moreover, the general scalar as well as vector equation governing diffraction management is derived from first principles based on asymptotic theory.

## 2. Waveguide array

As mentioned above, an array of coupled optical waveguides is a setting that represents a convenient laboratory for experimental observations and theoretical predictions. Such system (see [Fig. 1](#)) is typically composed of three layers of AlGaAs material: a substrate with refractive index  $n_0$ , a core with higher index ( $n_1$ ) and surface with index  $n_0$ . By etching the surface of the waveguide, one forms a periodic structure which is called a waveguide array. Self-trapping of light in the “y” (i.e., vertical) direction is possible (even in the linear regime) by virtue of the principle of total internal reflection. On the other hand, the beam will diffract in the “x”-direction unless it is

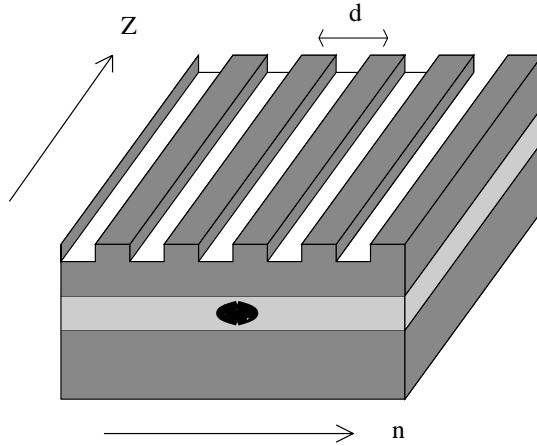


Fig. 1. AlGaAs waveguide structure. It is composed of three layers of AlGaAs material: a substrate with refractive index  $n_0$ , a core with higher index ( $n_1$ ) and surface with index  $n_0$ . By etching the surface of the waveguide, one forms a periodic structure which is called a waveguide array.

balanced by nonlinearity. In the following we describe the propagation of light in such a periodic structure both in the linear and nonlinear regimes.

### 2.1. Linear and nonlinear propagation

If the full width at half maximum (FWHM),  $\tau$ , of the optical field is small compared to the distance,  $d$ , between adjacent waveguides, then the propagating beams across each single waveguide do not “feel” each other. Therefore, the amplitude of each beam evolves independently according to the linear wave equation:

$$\frac{d^2 \psi_0}{dx^2} + [k_0^2 f_0^2(x) - \lambda_0^2] \psi_0 = 0, \tag{2.1}$$

where  $k_0$  is the wavenumber of the optical field in vacuum,  $f_0^2$  the refractive index of a single waveguide and  $\lambda_0$  the lowest eigenvalue (propagation constant) that corresponds to the ground state  $\psi_0$  (a bell shape eigenfunction). In this respect we have assumed that a single waveguide supports only a single mode. The more intricate situation of multimode waveguide is also possible in which case  $\lambda_0 \rightarrow \lambda_j$  and  $\psi_0 \rightarrow \psi_j$  where  $j$  is the number of modes occupied by a single waveguide. On the other hand when  $\tau$  is on the order of  $d$  or larger, then there is a significant overlap between modes of adjacent waveguide (see Fig. 2). In either case, the beam’s amplitude is not constant in  $z$  anymore. Moreover, when the intensity of the incident beam is sufficiently high then the refractive index of the medium will depend on the intensity which for Kerr media is proportional to the intensity. In this case, the evolution of the total field’s amplitude  $\Psi$  follows from Maxwell equations (see details in Section 5.3):

$$\left( \frac{\partial^2}{\partial z^2} + \frac{\partial^2}{\partial x^2} \right) \Psi + (k_0^2 f^2(x) + \delta |\Psi|^2) \Psi = 0, \tag{2.2}$$

where  $f^2(x)$  represents the refractive index of the entire structure and  $\delta$  a small parameter to be determined later. If the overlap between adjacent modes is “small”, which is valid in the regime  $\mu \equiv \tau/d \ll 1$ , we expect the power exchange to be slow. By introducing a slow scale  $Z = \varepsilon z$  ( $\varepsilon$  is a small parameter to be determined later) we

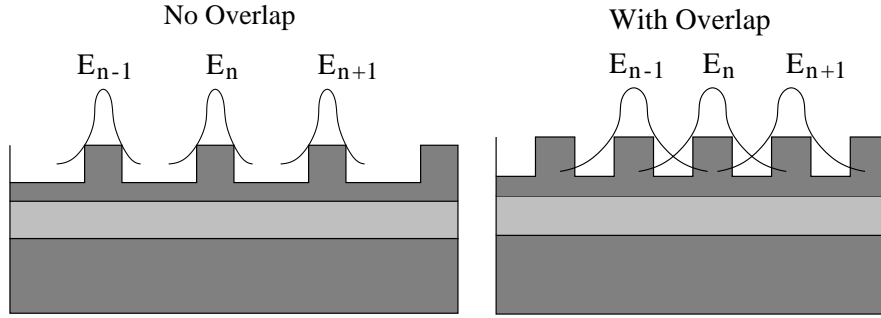


Fig. 2. Cross-section of the waveguide array and mode overlap.

approximate the solution to Eq. (2.2) as a multiscale perturbation series:

$$\Psi = \sum_{m=-\infty}^{+\infty} E_m(Z)\psi_m(x) \exp(-i\lambda_0 z). \tag{2.3}$$

In this notation,  $\psi_m(x) = \psi_0(x - md)$  and  $f_m^2(x) = f_0^2(x - md)$ . Substituting the ansatz (2.3) into Eq. (2.2), we find

$$\sum_{m=-\infty}^{+\infty} \left[ -2i\varepsilon\lambda_0\psi_m \frac{\partial E_m}{\partial Z} + \varepsilon^2 \psi_m \frac{\partial^2 E_m}{\partial Z^2} + \left( \frac{d^2\psi_m}{dx^2} + k_0^2 f^2 \psi_m - \lambda_0^2 \psi_m \right) E_m + \delta \sum_{m',m''} E_m E_{m'} E_{m''}^* \psi_m \psi_{m'} \psi_{m''}^* \right] e^{-i\lambda_0 z} = 0. \tag{2.4}$$

Using Eq. (2.1) in the above equation, multiplying Eq. (2.4) by  $\psi_n^* \exp(i\lambda_0 z)$  and integrating over  $x$  yields the following:

$$\sum_{m=-\infty}^{+\infty} \left[ \left( -2i\varepsilon\lambda_0 \frac{\partial E_m}{\partial Z} + \varepsilon^2 \frac{\partial^2 E_m}{\partial Z^2} \right) \int_{-\infty}^{+\infty} dx \psi_m \psi_n^* + k_0^2 E_m \int_{-\infty}^{+\infty} dx \Delta f_m^2 \psi_m \psi_n^* + \delta \sum_{m',m''} E_m E_{m'} E_{m''}^* \int_{-\infty}^{+\infty} dx \psi_n^* \psi_m \psi_{m'} \psi_{m''}^* \right] = 0. \tag{2.5}$$

Here,  $\Delta f_m^2 \equiv f^2 - f_m^2$  which measures the deviation of the total refractive index from each individual waveguide. As mentioned earlier, the overlap integral between adjacent waveguides is an important measure in determining the dynamic evolution of the modes. With this in mind we shall *assume* that the overlap integrals appearing in Eq. (2.5) can be approximated by

$$\int dx \psi_m \psi_{m+N}^* = a_N \varepsilon^N, \quad \int dx \Delta f_m^2 |\psi_m|^2 = c_0 \varepsilon, \quad \int dx \Delta f_m^2 \psi_m^* \psi_{m\pm 1} = c_1 \varepsilon. \tag{2.6}$$

In order to understand the idea behind this scaling, we will assume that the mode at waveguide  $m$  can be modeled by

$$\psi_m(x) = \operatorname{sech} \kappa(x - md), \tag{2.7}$$

where  $\kappa = 1/\tau$  and  $\tau$  is the FWHM. The reason for this choice is only to simplify the analysis. In fact, the real modes of a step index waveguide has exponential behavior which is close to a sech-like mode. Other choices of eigenfunctions with different exponential decays are possible, e.g.,  $\psi_m(x) = \exp[-(x - md)^2/\tau^2]$  but the basic ordering mechanism remains the same. A straightforward calculation shows that

$$\int_{-\infty}^{+\infty} dx \psi_m \psi_n^* = c e^{-|n-m|/\mu} \tag{2.8}$$

with  $c$  being a constant of order 1. Since  $\mu \ll 1$ , then the choice  $\varepsilon = \exp(-1/\mu)$  provides a measure for the order of magnitude for the overlap integral. Restricting the sum in Eq. (2.5) to nearest neighbors, i.e.,  $m = n, n \pm 1$  (which contribute to the order  $\varepsilon$  equation) and assuming that the only order 1 contribution comes from the nonlinear term is when  $m = n = m' = m''$  and that

$$\int_{-\infty}^{+\infty} dx |\psi_n|^4 = g_{nl},$$

we find that to  $O(\varepsilon)$  the nonlinear evolution of  $E_n$  is given by

$$-2i\lambda_0 a_0 \frac{\partial E_n}{\partial Z} + k_0^2 c_0 E_n + k_0^2 c_1 (E_{n+1} + E_{n-1}) + g_{nl} |E_n|^2 E_n = 0, \tag{2.9}$$

where we have taken  $\delta = \varepsilon$  to ensure maximal balance. By defining a new variables  $\tilde{z} = Z/(2\lambda_0 a_0)$ ,  $k_0^2 c_1 = C$ ,  $E_n = \tilde{E}_n^* \exp(-ik_0^2 c_0 \tilde{z})$  we find that  $\tilde{E}_n$  satisfies (dropping the tilde)

$$i \frac{\partial E_n}{\partial z} + C(E_{n+1} + E_{n-1}) + g_{nl} |E_n|^2 E_n = 0. \tag{2.10}$$

To put the DNLS equation in dimensionless form, we define

$$E_n = \sqrt{P_*} \phi_n \exp(2iCz), \quad z' = \frac{z}{z_{nl}} \tag{2.11}$$

with  $P_*$  and  $z_{nl}$  being the characteristic power and  $z_{nl}$  the nonlinear length scale. Then  $\phi_n$  satisfies

$$i \frac{d\phi_n}{dz} + \frac{1}{h^2} (\phi_{n+1} + \phi_{n-1} - 2\phi_n) + |\phi_n|^2 \phi_n = 0 \tag{2.12}$$

with  $z_{nl}C = 1/h^2$  and  $z_{nl} = 1/(g_{nl}P_*)$ . In the DNLS equation there are two important length scales: the diffraction and nonlinear length scales, respectively, defined by  $L_D \sim 1/C$  and  $z_{nl} = 1/(g_{nl}P_*)$ . Solitons which are self-confined and invariant structures are expected to form when  $L_D \sim z_{nl}$ .

### 2.2. New discrete nonlinear Schrödinger type equation

We begin as before with the nonlinear Helmholtz equation with modulated Kerr coefficient:

$$\left( \frac{\partial^2}{\partial z^2} + \frac{\partial^2}{\partial x^2} \right) \Psi + (k_0^2 f^2(x) + \delta(x) |\Psi|^2) \Psi = 0, \tag{2.13}$$

where  $f^2(x)$  is defined before, and  $\delta(x)$  measures the local change of nonlinear refractive index along the transverse direction. Importantly, note that as compared to Eq. (2.2), we now assume the nonlinear coefficient to be a spatially dependent function. Moreover, we shall assume here, that the nonlinear index change  $\delta(x)$  is an odd function relative to each waveguide (i.e.,  $\delta(x) \rightarrow \delta(x - nd) = -\delta(-x + nd)$ ). Following the reasoning outlined before, we

approximate the solution to Eq. (2.13) via a multiscale perturbation series given in Eq. (2.3). In this case, the linear part remains the same but the nonlinear contribution changes to

$$\mathcal{N} = \sum_{m=-\infty}^{+\infty} \sum_{m', m''} E_m E_{m'} E_{m''}^* \delta(x) \psi_m \psi_{m'} \psi_{m''}^* e^{-i\lambda_0 z}. \quad (2.14)$$

Multiplying Eq. (2.14) by  $\psi_n^* \exp(i\lambda_0 z)$  and integrating over  $x$  yields the following:

$$\mathcal{I} = \int_{-\infty}^{+\infty} dx \mathcal{N} \psi_n^* \exp(i\lambda_0 z) = \sum_{m=-\infty}^{+\infty} \sum_{m', m''} E_m E_{m'} E_{m''}^* \int_{-\infty}^{+\infty} dx \delta(x) \psi_n^* \psi_m \psi_{m'} \psi_{m''}^*. \quad (2.15)$$

Since  $\delta(x)$  is an odd function then there is no on-site contribution, i.e.:

$$\mathcal{I}_{m=m'=m''=n} = |E_n|^2 E_n \int_{-\infty}^{+\infty} dx \delta(x) |\psi_n|^4 = 0.$$

Therefore, the leading order contribution comes by setting  $m = n \pm 1, m' = m'' = n; m = m'' = n, m' = n \pm 1; m = m' = n, m'' = n \pm 1$ . The nonlinearity in each of the cases is

$$\begin{aligned} \mathcal{I}_{m=n\pm 1, m'=m''=n} &= \mathcal{I}_{m=m''=n, m'=n\pm 1} = \pm |E_n|^2 E_{n\pm 1} \int_{-\infty}^{+\infty} dx \delta(x) \psi_n^* |\psi_n|^2 \psi_{n\pm 1}, \\ \mathcal{I}_{m=m'=n, m''=n\pm 1} &= \pm E_n^2 E_{n\pm 1}^* \int_{-\infty}^{+\infty} dx \delta(x) |\psi_n|^2 \psi_n \psi_{n\pm 1}^*. \end{aligned}$$

The linear portion follows the same derivation as in Section 2.1 and we shall assume that the waveguide function  $f^2(x)$  is  $O(\varepsilon)$ , and  $Z = \varepsilon^2 z, \delta(x) = O(\varepsilon)$ . Combining all the linear and nonlinear terms, we find

$$\begin{aligned} -2i\lambda_0 a_0 \varepsilon^2 \frac{\partial E_n}{\partial Z} + k_0^2 c_0 \varepsilon E_n + k_0^2 c_1 \varepsilon^2 (E_{n+1} + E_{n-1}) + 2Q_1 \varepsilon^2 |E_n|^2 (E_{n+1} - E_{n-1}) \\ + Q_2 \varepsilon^2 E_n^2 (E_{n+1}^* - E_{n-1}^*) = 0, \end{aligned} \quad (2.16)$$

where

$$\begin{aligned} a_0 &= \int_{-\infty}^{+\infty} dx |\psi_n(x)|^2, \quad c_0 \varepsilon = \int_{-\infty}^{+\infty} dx (f^2 - f_n^2) |\psi_n(x)|^2, \\ c_1 \varepsilon^2 &= \int_{-\infty}^{+\infty} dx (f^2 - f_{n+1}^2) \psi_n(x) \psi_{n+1}(x), \quad Q_1 \varepsilon^2 = \int_{-\infty}^{+\infty} dx \delta(x) |\psi_n(x)|^2 \psi_n^*(x) \psi_{n+1}(x), \\ Q_2 \varepsilon^2 &= \int_{-\infty}^{+\infty} dx \delta(x) |\psi_n(x)|^2 \psi_n(x) \psi_{n+1}^*(x). \end{aligned}$$

By defining new variables  $\tilde{z} = Z/(2\lambda_0 a_0), k_0^2 c_1 = C, E_n = \tilde{E}_n^* \exp(-ik_0^2 c_0 \tilde{z}/\varepsilon)$ , we find that  $\tilde{E}_n$  satisfies

$$i \frac{\partial \tilde{E}_n}{\partial \tilde{z}} + C(\tilde{E}_{n+1} + \tilde{E}_{n-1}) + 2Q_1 |\tilde{E}_n|^2 (\tilde{E}_{n+1} - \tilde{E}_{n-1}) + Q_2 \tilde{E}_n^2 (\tilde{E}_{n+1}^* - \tilde{E}_{n-1}^*) = 0. \quad (2.17)$$

### 2.3. Diffraction properties of a waveguide array

In this section we consider the basic properties of discrete diffraction of a linear array of waveguides emphasizing the recent discovery of anomalous diffraction [11]. However, we consider first propagation of light in bulk linear

and homogeneous media which is governed by the linear Helmholtz equation:

$$\nabla^2 \mathbf{E} + k^2 \mathbf{E} = 0, \quad \nabla^2 = \frac{\partial^2}{\partial x^2} + \frac{\partial^2}{\partial z^2}, \quad (2.18)$$

where  $\mathbf{E}$  is the amplitude of the electric field. If we assume a solution of the form  $\mathbf{E} = a \exp[i(k_z z + k_x x)]$  then we find  $k_z = \sqrt{k^2 - k_x^2}$ . In the paraxial approximation ( $k_x/k \ll 1$ ), the diffraction relation reads  $k_z \approx k - k_x^2/2k$ . Then the group velocity is defined by  $\partial k_z / \partial k_x \approx -k_x/k$  which says that each transverse component  $k_x$  travels at different rates hence beam will diffract. A measure for the rate of diffraction is  $\partial^2 k_z / \partial k_x^2$  which for plane waves is  $\approx -1/k < 0$ . Since all plane waves have this definite negative sign for diffraction, it is referred to as normal diffraction regime. Note that this is exactly the opposite from dispersion in which the normal regime is positive. Next, we discuss linear propagation of light in a waveguide array. As mentioned in Section 2.1, the dynamics of the beam's amplitude  $E_n(z)$  at waveguide number  $n$  follows Eq. (2.10). In this case, when an extended state or cw mode of the form

$$E_n(z) = A \exp[i(k_z z - n k_x d)] \quad (2.19)$$

is inserted into Eq. (2.10) it yields the following diffraction relation:

$$k_z = 2C \cos(k_x d). \quad (2.20)$$

In close analogy to the definition of dispersion, discrete diffraction is given by  $k_z'' = -2Cd^2 \cos(k_x d)$ . Since the diffraction relation is periodic in Fourier space, we shall restrict the discussion for wavenumbers in the interval  $|k_x d| \leq \pi$ . In that region, the diffraction is *normal* for wavenumbers  $k_x$  satisfying  $-\pi/2 < k_x d \leq \pi/2$  ( $k_z'' < 0$ ) and is *anomalous* in the range  $\pi/2 < |k_x d| \leq \pi$ . Moreover, contrary to the bulk case, diffraction can even vanish when  $k_x d = \pm\pi/2$ . In practice, the sign and value of the diffraction can be controlled and manipulated by launching light at a particular angle  $\gamma$  or equivalently by tilting the waveguide array. The relation between  $k_x$ ,  $k_z$  and the tilt angle is given by  $\sin \gamma = k_x/k$ . This in turn allows the possibility of achieving a “self-defocusing” (with *positive* Kerr coefficient) regime which leads to the formation of discrete dark solitons [28]. To understand more about diffraction management we consider three typical cases for which light enters the central waveguide array at different angles, say,  $k_x d = 0, \pi/2$  and  $\pi$ . When  $k_x d = 0$  then light tunnels between adjacent waveguides giving rise to discrete diffraction. The phase front in this case has a concave (negative) curvature. On the other hand, if  $k_x d = \pi$ , then diffusion of light still occurs but this time the phase front has convex (positive) curvature. Finally, at  $k_x d = \pi/2$  the diffraction vanishes (even though light can couple to different waveguides) and in the absence of any higher order diffraction the phase front looks almost flat (see Fig. 3).

### 3. Stationary and moving solitons: Fourier transform method

In this section, we introduce a new method to obtain both stationary and moving solitons for the DNLS equation. The essence of the method is to transform the DNLS equation governing the solitary wave into Fourier space, where the wave function is smooth, and then deal with a nonlinear nonlocal integral equation for which we employ a rapidly convergent numerical scheme to find solutions. A key advantage of the method is to transform a differential-delay equation into an integral equation for which computational methods are effective (see also Refs. [42,43]). Mathematically, the method also provides a foundation upon which an analytic theory describing solitons in nonlinear lattices can be constructed. Moreover, the method is applicable to continuous problems.

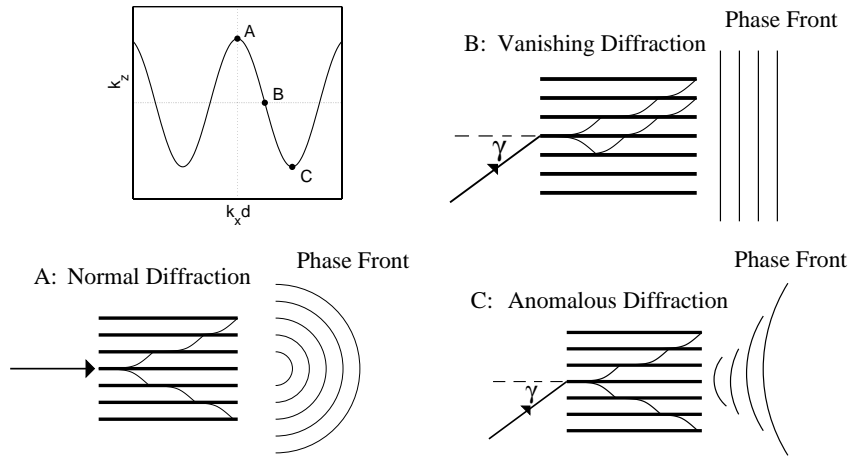


Fig. 3. Diffraction relation (top left) showing three typical examples of diffraction scenarios: (A) Normal in which the phase front is concave; (B) vanishing diffraction in which the phase front is almost flat; (C) anomalous diffraction with convex phase front.

### 3.1. Stationary solutions

We look for a stationary solution to Eq. (2.12) in the form

$$\phi_n = F_n \exp(i\omega z) \tag{3.1}$$

with  $F_n$  being real valued function and  $\omega$  a real eigenvalue. Then  $F_n$  satisfies

$$-\omega F_n + \frac{1}{h^2}(F_{n+1} + F_{n-1} - 2F_n) + F_n^3 = 0. \tag{3.2}$$

Eq. (3.2) can be solved using Newton iteration scheme by which one gives initial values for  $F_0$  and  $F_1$  and then iterate. However, our aim here is to provide a different approach based on the Fourier transform method in which a discrete equation is transformed into an integral equation. To this end, we use the transform defined by

$$\hat{u}(w, t) = \sum_{n=-\infty}^{+\infty} u_n w^{-n} \tag{3.3}$$

with the inverse transform given as

$$u_n(t) = \frac{1}{2\pi i} \oint_{C_0} \hat{u}(w, t) w^{n-1} dw, \tag{3.4}$$

where  $w$  is a complex number and  $C_0$  the unit circle. If we let  $w = e^{iqh}$  then Eq. (3.4) coincides with the discrete Fourier transform

$$\hat{u}(q) = \sum_{m=-\infty}^{+\infty} u_m e^{-iqmh}, \quad u_m = \frac{h}{2\pi} \int_{-\pi/h}^{\pi/h} \hat{u}(q) e^{iqmh} dq. \tag{3.5}$$

Applying the discrete Fourier transform in Eq. (3.2) leads to the following nonlinear integral equation:

$$\hat{F}(q) = \frac{h^2}{4\pi^2 \Omega(q)} \iint_{\mathbb{D}^2} dq_1 dq_2 \hat{F}(q_1) \hat{F}(q_2) \hat{F}(q - q_1 - q_2) \equiv \mathcal{K}_\omega[\hat{F}(q)], \tag{3.6}$$

where  $\mathbb{D}^2 = \mathbb{D} \times \mathbb{D}$  and  $\mathbb{D} = [-\pi/h, \pi/h]$ . Here,  $\Omega(q) = \omega + 2(1 - \cos(hq))/h^2$  corresponds to the frequency of the linear excitations. The important conclusion is that the soliton can be viewed as a fixed point of an infinite-dimensional nonlinear functional. To numerically find the fixed point, one might start with an initial guess for  $\hat{F}(q)$  and iterate Eq. (3.6) using

$$\hat{F}_{n+1}(q) = \mathcal{K}_\omega[\hat{F}_n(q)], \quad n \geq 0. \tag{3.7}$$

However, if the norm of  $\hat{F}(q)$  is “large” then the iteration based on Eq. (3.7) will diverge while it will converge to zero for small norm. This is because the right hand side of Eq. (3.7) has degree 3 whereas the left hand side is suggested of degree 1. To overcome this difficulty, we employ instead, a modified Neumann iteration scheme and consider a new equation

$$\hat{F}_{n+1}(q) = \left( \frac{\langle \hat{F}_n, \hat{F}_n \rangle}{\langle \hat{F}_n, \mathcal{K}_\omega \rangle} \right)^{3/2} \mathcal{K}_\omega[\hat{F}_n(q)], \quad n \geq 0, \tag{3.8}$$

where the inner product  $\langle \cdot \rangle$  is defined by

$$\langle \hat{f}, \hat{g} \rangle \equiv \int_{\mathbb{D}} \hat{f}(q)\hat{g}(q) \, dq. \tag{3.9}$$

The factor 3/2 is chosen to make the right hand side of Eq. (3.8) of degree 0 which yields convergence of the scheme [42,43]. When  $F_m$  is real and even, it implies that  $\hat{F}(q)$  is also real. Clearly when  $\hat{F}_n(q) \rightarrow \hat{F}_s(q)$  as  $n \rightarrow \infty$  then  $\langle \hat{F}_n, \hat{F}_n \rangle / \langle \hat{F}_n, \mathcal{K}_\omega \rangle \rightarrow 1$  and in turn  $\hat{F}_s(q)$  will be the solution to Eq. (3.6). Fig. 4 shows a typical solution to (3.6) both in the Fourier domain (Fig. 4a) and in physical space (Fig. 4b) for different values of lattice spacing  $h$ . The proposed scheme converges linearly as can be seen in Fig. 5 where the relative error between successive iterations  $E_n^F$  defined by

$$E_n^F = \log |E_n - E_{n-1}| \tag{3.10}$$

is plotted for different values of lattice spacing  $h$  and typical parameter value  $\omega = 1$ . In order to shed more light on the property of the solution, we will consider for comparison the IDNLS given by [40]

$$i \frac{\partial u_n}{\partial t} + \frac{1}{h^2}(u_{n+1} + u_{n-1} - 2u_n) + |u_n|^2(u_{n+1} + u_{n-1}) = 0, \tag{3.11}$$

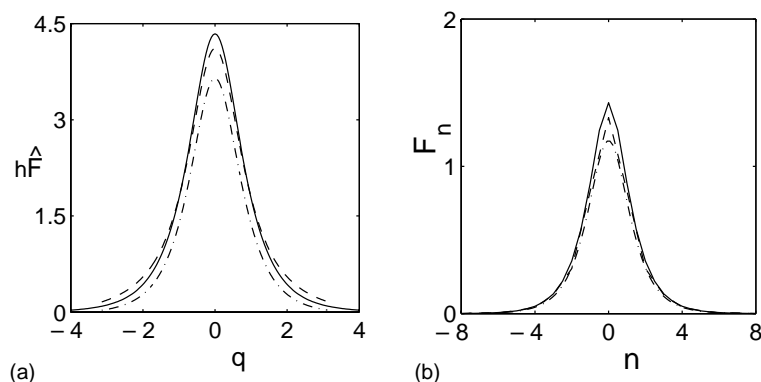


Fig. 4. Mode profiles obtained with  $\omega = 1$  in Fourier space (a), for  $h = 0.5$  (solid),  $h = 1$  (dashed) and  $h = 1$  (dashed-dotted) for the integrable case. (b) Soliton shape in physical space for  $h = 0.5$  (solid),  $h = 1$  (dashed) and for the integrable case at  $h = 1$  (dashed-dotted).

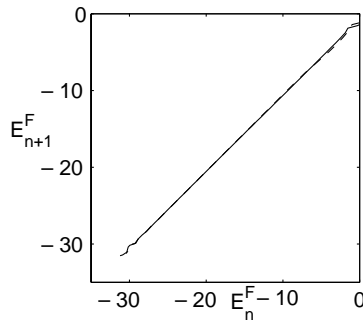


Fig. 5. Plot of the relative error  $E_n^F$  between successive iterations for  $h = 0.5$  (solid) and  $h = 1$  (dashed) with  $\omega = 1$ .

which possesses an exact TW solution of the form

$$u_n(t) = \frac{\sin(h)}{h} \operatorname{sech}(nh - Vt) \exp[-i(\beta nh - \omega t)], \tag{3.12}$$

$$\omega = \frac{2}{h^2} [\cos(\beta h) \cos(h) - 1], \quad V = -\frac{2}{h^2} \sin(\beta h) \sin(h). \tag{3.13}$$

Consider first the case when the soliton is stationary ( $V = 0$ ). The method of discrete Fourier transform rapidly converges when applied to Eq. (3.11) and agrees with Eq. (3.12) (see Fig. 4). What is also remarkable about the solution (3.12) is that it forms a *continuous* function, i.e., the solution is not only defined at the grid points  $n = 0, \pm 1, \pm 2, \dots$  but also it can be defined off the grid points (e.g.,  $n = 1.234$ ). This suggests that Eq. (3.11) can be embedded in a larger class of differential-delay equations in which the discrete variable  $n$  can be considered as a *continuous* variable without affecting the solution. With this extension in mind, we could search for stationary solutions for Eq. (3.11) (with  $n \equiv \xi$  being a continuous variable) by applying the continuous Fourier transform:

$$\hat{u}(q) = \int_{-\infty}^{+\infty} u(\xi) e^{-iq\xi} d\xi, \quad u(\xi) = \frac{1}{2\pi} \int_{-\infty}^{+\infty} \hat{u}(q) e^{iq\xi} dq, \tag{3.14}$$

which can be obtained from Eq. (3.5) by taking the limit  $h \rightarrow 0$  with fixed  $nh = \xi$ . The important question we ask is: does a continuous stationary solution exist for the DNLS equation as well? To partially answer this question we applied the continuous Fourier transform in Eq. (3.2) (to find stationary solution). The only change from Eq. (3.6) is that  $\mathbb{D}^2 \rightarrow \mathbb{R}^2$ . We found that the numerical scheme based on (3.8) does not converge which indicates that a continuous stationary localized solution to the DNLS may not exist. On the other hand we did find numerically that a continuous Fourier transform solution to Eq. (3.11) converged rapidly. As we will see later, this will have a direct impact on the TW problem.

### 3.2. Remarks

Below we make some comments on the proposed scheme for discrete systems outlining its usefulness.

- The numerical scheme based on Eq. (3.8) can be replaced by one in which the convergent factors belong to  $L^1$ :

$$\|\hat{F}\|_1 \equiv \int_{\mathbb{D}} \hat{F}(q) dq. \tag{3.15}$$

In this case, the iteration scheme takes the form

$$\hat{F}_{n+1}(q) = \left( \frac{\|\hat{F}_n\|_1}{\|\mathcal{K}_\omega\|_1} \right)^{3/2} \mathcal{K}_\omega[\hat{F}_n(q)], \quad n \geq 0. \tag{3.16}$$

- Finding stationary solutions for multidimensional continuous partial differential equations (PDEs) using the above scheme is straightforward.
- Applying the Fourier transform technique to higher order continuous or discrete systems only results in a modification of the linear dispersion relation from, e.g.,  $\cos(qh) \rightarrow \cos(qh) + \cos(2qh)$ .
- The proposed technique is natural for diffraction-managed systems in which an infinite-dimensional nonlinear integral equation must be solved. Applying direct methods such as Newton iteration would be difficult on such diffraction-managed equations.

### 3.3. Numerical iteration based on energy renormalization

We next highlight a different approach based on energy renormalization to solve Eq. (3.6). As we have seen before, one reason why simple iteration scheme does not converge is because the right and left hand side of (3.6) have different homogeneity. An alternative method is to renormalize the wave function  $\hat{F}(q)$  at each iteration stage by its  $L^\infty$  (maximum) or  $L^2$  norm, respectively, defined by

$$\|\hat{F}\|_\infty \equiv \max_{q \in \mathbb{D}} |\hat{F}(q)|, \tag{3.17}$$

$$\|\hat{F}\|_2 \equiv \left( \int_{\mathbb{D}} |\hat{F}(q)|^2 dq \right)^{1/2}. \tag{3.18}$$

In this case the beam amplitude remains always finite. For discrete problems, the choice of the maximum norm is particularly natural since the problem is restricted to a finite domain in  $q$  space. To implement this scheme, we start with a localized guess,  $\hat{F}_0(q)$  and compute its norm  $\|\hat{F}_0\|$  (by  $\|\cdot\|$  we mean either  $\|\cdot\|_\infty$  or  $\|\cdot\|_2$ ). We then define the renormalized function  $\hat{\mathcal{F}}_0(q) = \hat{F}_0(q)/\|\hat{F}_0\|$ . Then from Eq. (3.6) we compute  $\hat{F}_1(q)$  and, in general, the  $m$ th iteration takes the form

$$\hat{F}_{m+1}(q) = \frac{h^2}{4\pi^2 \Omega(q)} \iint_{\mathbb{D}^2} dq_1 dq_2 \hat{\mathcal{F}}_m(q_1) \hat{\mathcal{F}}_m(q_2) \hat{\mathcal{F}}_m(q - q_1 - q_2), \tag{3.19}$$

$$\hat{\mathcal{F}}_m(q) = \frac{\hat{F}_m(q)}{\|\hat{F}_m\|}. \tag{3.20}$$

Note that as  $m \rightarrow \infty$  the scheme based on Eq. (3.20) converges, i.e.:

$$\lim_{m \rightarrow \infty} \|\hat{\mathcal{F}}_m - \hat{\mathcal{F}}_s\| = 0, \tag{3.21}$$

where  $\hat{\mathcal{F}}_s$  and  $\hat{F}_s = \|\hat{\mathcal{F}}_s\| \hat{\mathcal{F}}_s$  is the exact solution to Eq. (3.20). Importantly, Eq. (3.6) admits the following scaling property: if  $\hat{F}(q) = \varkappa \hat{F}'(q)$  then  $\hat{F}'(q) = \varkappa^2 \mathcal{K}_\omega[\hat{F}'(q)]$  is also a solution. In light of this scaling property we find that  $\hat{\mathcal{F}}_s$  and  $\hat{F}_s$  are also solutions to Eq. (3.6). We have compared the solution obtained by this method with the previous technique and with the IDNLS solution and found excellent agreement.

### 3.4. Do discrete TWs exist or not?

Finding analytical TW solutions for a continuous PDE and for differential-delay equations in particular, is a challenging problem. For some PDEs, TWs can be readily obtained by making use of either Galilean or Lorentz

invariance. However, for general discrete systems, such a symmetry does not exist. An additional source of difficulty that arises when dealing with differential-delay systems is the lack of quadrature. In this section, we describe a method to obtain TW solutions for discrete systems which is applicable to many discrete models such as FPU lattice, sine-Gordon to name a few. However, here we will focus our attention to TW of the DNLS model. Unlike the IDNLS in which exact continuous traveling solitons are known, there are no known explicit solutions for DNLS solitons. Previous studies of TWs for the DNLS equation employed various techniques and ansatz [44–46]. One method is to write the DNLS as a perturbed IDNLS [47] and use perturbation theory, based on inverse scattering, to gain some insight to the solution. However, this method is limited to moderately confined wave functions and cannot be used as a constructive method. Another technique is to use the “exact” stationary solutions discussed in Section 3.2 and, based on what we know from continuous NLS theory, employ a linear phase tilt:

$$\phi_n = F_n \exp(i\beta nh) \quad (3.22)$$

with  $F_n$  being the stationary solution found before and  $\beta$  the beam “velocity” or phase tilt. However, by doing so, we do not obtain a uniformly moving solitary wave (as can be seen in Fig. 6 where the top of the beam oscillates). This is even more clear when we zoom in on small amplitude where radiation modes are seen to be emitted during propagation (see Fig. 7). Our analysis, which is based on the discrete Fourier methods, reveals another fundamental distinction from the IDNLS traveling solitons: there are approximate TW solutions which are “multimode” discrete solitons, i.e., a single mode (sech-like shape) does not propagate without significant radiation [48]. In fact the modes we found are characterized by having a nonlinear “chirp”. To formulate the analysis, we look for traveling localized modes in the form

$$\phi_n(z) = u(\xi) \exp[-i(\beta nh - \omega z)], \quad \xi = nh - Vz \quad (3.23)$$

with  $V$  and  $\omega$  being the soliton velocity and wavenumber shift, respectively. Assuming  $u$  is complex, i.e.,  $u(\xi) = F(\xi) + iG(\xi)$  (with  $F, G$  being real), then Eq. (2.12) takes the form

$$V \frac{dG}{d\xi} + \mathcal{D}_1 F + \mathcal{D}_2 G + (F^2 + G^2)F = \omega F, \quad -V \frac{dF}{d\xi} + \mathcal{D}_1 G - \mathcal{D}_2 F + (F^2 + G^2)G = \omega G, \quad (3.24)$$

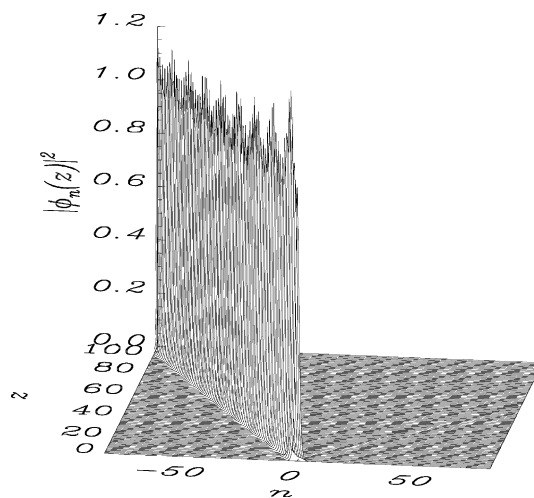


Fig. 6. Evolution of the stationary solution in physical domain for  $\omega = 1$  and  $h = 0.5$  obtained by direct numerical simulation by employing a linear phase tilt (or velocity) with  $\beta = 0.5$ .

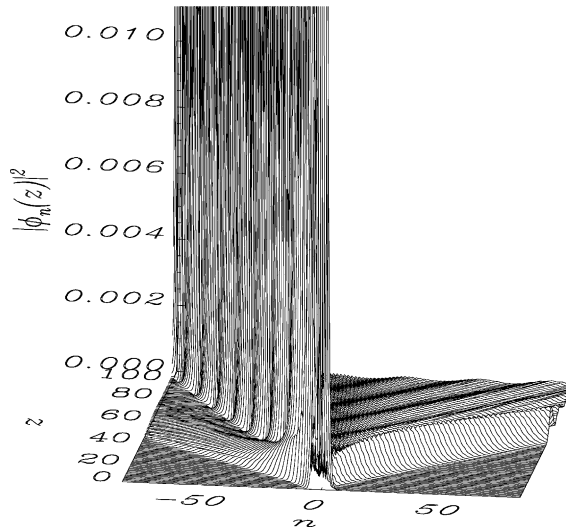


Fig. 7. The same as in Fig. 6 but zoomed to small amplitude. Radiation modes are clearly seen which leads to a nonuniform moving beam.

where the linear operators  $\mathcal{D}_1$  and  $\mathcal{D}_2$  are defined by

$$\mathcal{D}_1 f \equiv \frac{1}{h^2} [\cos(\beta h)(E_+ + E_-)f - 2f], \quad \mathcal{D}_2 g \equiv \frac{\sin(\beta h)}{h^2} (E_+ - E_-)g \tag{3.25}$$

with  $E_{\pm}S(\xi) \equiv S(\xi \pm h)$ . To find the mode shapes and soliton velocity, we proceed as before by taking the discrete Fourier transform of Eq. (3.24) which yields the following iteration scheme:

$$\hat{F}_{n+1}(q) = \frac{\Omega_2(q)}{\Omega_1(q)} \tilde{G}_n(q) + \left(\frac{\alpha_1}{\beta_1}\right)^{3/2} \mathcal{Q}_1[\hat{F}_n, \tilde{G}_n], \quad \tilde{G}_{n+1}(q) = \frac{\Omega_2(q)}{\Omega_1(q)} \hat{F}_n(q) + \left(\frac{\alpha_2}{\beta_2}\right)^{3/2} \mathcal{Q}_2[\hat{F}_n, \tilde{G}_n], \tag{3.26}$$

where  $\hat{F}(q)$  and  $\hat{G}(q) \equiv -i\tilde{G}(q)$  are the Fourier transforms of  $F(\xi)$  and  $G(\xi)$ , respectively, and

$$\mathcal{Q}_1[\hat{F}, \tilde{G}] = \frac{h^2}{4\pi^2\Omega_1(q)} (\hat{F} * \hat{F} * \hat{F} - \tilde{G} * \tilde{G} * \hat{F}), \quad \mathcal{Q}_2[\hat{F}, \tilde{G}] = \frac{h^2}{4\pi^2\Omega_1(q)} (\hat{F} * \hat{F} * \tilde{G} - \tilde{G} * \tilde{G} * \tilde{G}), \tag{3.27}$$

where  $*$  denotes a convolution:

$$f * g = \int_{\mathbb{D}} f(k)g(q - k) dk.$$

The convergence factors  $\alpha_j$  and  $\beta_j$ ,  $j = 1, 2$  are given by

$$\alpha_1 = \left\langle \hat{F}_n, \hat{F}_n - \frac{\Omega_2 \tilde{G}_n}{\Omega_1} \right\rangle, \quad \alpha_2 = \left\langle \tilde{G}_n, \tilde{G}_n - \frac{\Omega_2 \hat{F}_n}{\Omega_1} \right\rangle, \quad \beta_1 = \langle \hat{F}_n, \mathcal{Q}_1 \rangle, \quad \beta_2 = \langle \tilde{G}_n, \mathcal{Q}_2 \rangle$$

with

$$\Omega_1(q) = \omega + \frac{2}{h^2} [1 - \cos(hq) \cos(\beta h)], \quad \Omega_2(q) = \frac{2}{h^2} \sin(hq) \sin(\beta h) + Vq. \tag{3.28}$$

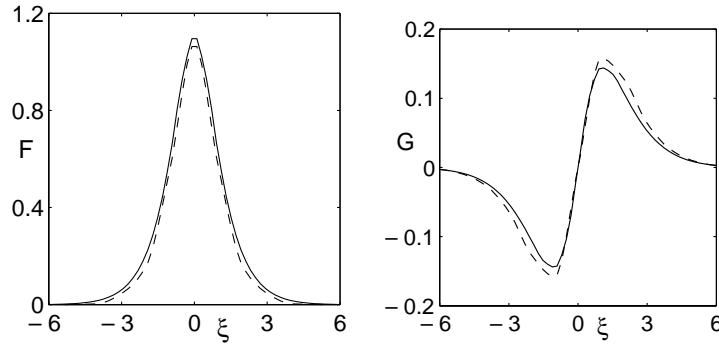


Fig. 8. Mode shapes in physical space for  $\omega = 1$  and  $\beta = 0.5$ . Solid line corresponds to  $h = 0.5$  and velocity  $V = -0.25$  whereas dashed line for  $h = 1$  and  $V = -0.155$ .

The next stage would be to iterate Eq. (3.26). However, Eq. (3.26) form a system of two equations with *three* unknowns,  $\hat{F}$ ,  $\tilde{G}$  and  $V$ . Therefore, we need to add an extra condition to match the number of variables with the number of equations. By doing so, we proceed as follows. For a given set of parameters  $h$ ,  $\omega$  and  $\beta > 0$ , the mode shapes and soliton velocity are found by iterating Eq. (3.26) with an initial guess, e.g.,  $\hat{F}_0(q) = \text{sech}(q)$ ,  $\tilde{G}_0(q) = \text{sech}(q) \tanh(q)$  and  $V = V_* < 0$ . The iterations are carried out until the condition  $|\mathcal{E}_j| \equiv |\alpha_j - \beta_j| < \epsilon$  ( $j = 1, 2$ ) is satisfied with  $\epsilon > 0$  being a prescribed tolerance. However, unlike the stationary case, here, the soliton velocity is still to be determined. For any choice of  $V_* < 0$  if  $|\mathcal{E}_j| \not< \epsilon$ , we seek a different value of  $V_*$  at which  $\mathcal{E}_j$  changes sign. Then, we use the bisection method to change  $V_*$  in order to locate the correct velocity  $V$  and modes  $\hat{F}$ ,  $\tilde{G}$  for each  $\omega$ ,  $\beta$  and  $h$ . Typical soliton modes are shown in Fig. 8.

At this stage it is useful to make some further comments on the Fourier transform. Since  $\xi$  is a continuous variable it implies that Eq. (3.24) are continuous equations in  $\xi$ . Therefore it seems natural to use the *continuous* Fourier transform rather than discrete. However, when we apply the *continuous* Fourier transform in Eq. (3.24), we find that the numerical scheme based on Eq. (3.26) with  $\pi/h \rightarrow \infty$  does not converge to a solution. This is a strong indication that, as opposed to the integrable case, a *true continuous* stationary or TW solutions to the DNLS model does not exist. By continuous solution we mean a solution that can be defined off the lattice points which is *necessary* when discussing TWs on lattices. In fact, the perturbation analysis presented below supports this observation as it *fails* to give consistent results off the grid points. To support these founding, let us take the continuous limit on the DNLS which yields

$$i \frac{\partial \phi}{\partial z} + \phi_{xx} + \alpha_4 \phi_{xxx} + |\phi|^2 \phi = 0, \quad (3.29)$$

where  $\alpha_4 = h^2/12$ . Importantly, it was shown in [49] that Eq. (3.29) with  $\alpha_4 > 0$  lacks exact soliton solutions whereas it possess closed form solution for  $\alpha_4 < 0$  [50]. Moreover, in this case the asymptotic behavior of the solution to Eq. (3.29) in the limit  $0 < \alpha_4 \ll 1$  is [49]

$$\phi \sim \text{sech}(\xi) + O(e^{-\gamma/|h|})P(\xi, z),$$

with  $\xi = x - Vz$  and  $\gamma$  being a positive constant with  $P(\xi, z)$  being a concrete function of *both*  $\xi$  and  $z$  (see Eq. (16) of Ref. [49]). This means that for  $h = 0.1$  (as an example), the nonstationary correction to the exact solution (when  $\alpha_4 = 0$ ) is exponentially small and cannot be captured in numerical simulations. These results differ from those of [51,52] in which a “continuous” traveling solitary waves were reported using Fourier series expansions with finite period  $L$  while *assuming convergence* as  $L \rightarrow \infty$ .

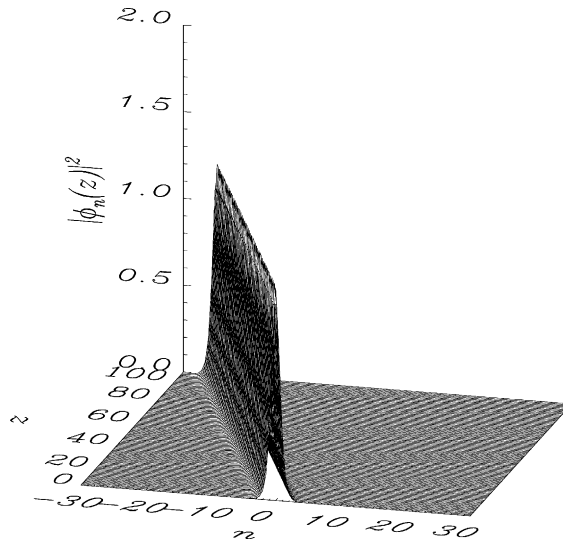


Fig. 9. Evolution of a moderately localized soliton in physical domain for  $\beta = 0.5$ ,  $V = -0.25$ ,  $\omega = 1$  and  $h = 0.5$  obtained by direct numerical simulation.

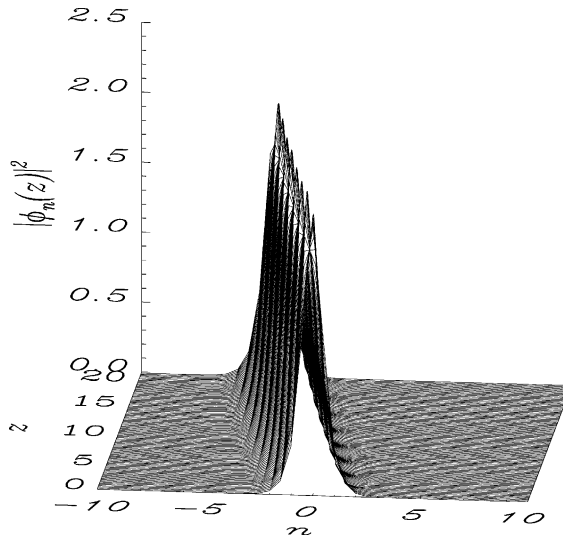


Fig. 10. Evolution of a strongly localized soliton in physical domain for  $\beta = 0.5$ ,  $V = -0.2$ ,  $\omega = 2$  and  $h = 0.5$  obtained by direct numerical simulation.

Although Eq. (3.26) can be solved numerically with high accuracy, the resulting solutions are only obtained at the discrete locations  $\xi = nh$ , while all real values of  $\xi$  are called upon in a TW solution. So the question we want to ask is: what happen to the modes found above when they propagate across the arrays? To answer this question, we simulated Eq. (2.12) using  $\phi_n(z = 0) = u(nh) e^{-i\beta nh}$  as an initial condition with  $u(nh) = F_{TW}(nh) + iG_{TW}(nh)$  being the solutions obtained from (3.26). When a moderately localized mode<sup>1</sup> is launched, the beam moved across the

<sup>1</sup> Moderate localization obtains when the FWHM of the intensity is 4–6 lattice sites; strong localization occurs when FWHM = 1–3 lattice sites.

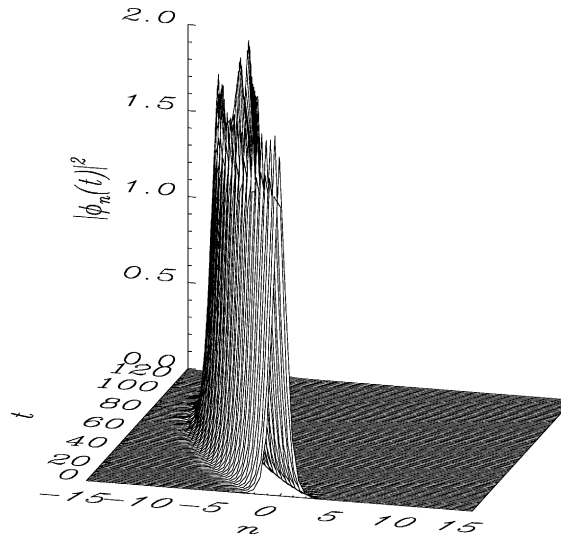


Fig. 11. Evolution of a strongly localized soliton in physical domain for large distance. Contrary to Fig. 10, in which the beam travels for short distance, here after some distance, the beam starts to decelerate. Parameters are:  $\beta = 0.5$ ,  $V = -0.2$ ,  $\omega = 2$  and  $h = 0.5$ .

waveguides undistorted (Fig. 9) over 100 normalized  $z$ -units. This corresponds, according to the experimental data reported in [11], to 120 mm (recall that the waveguides used in [11] were 6 mm in length). On the other hand, strongly localized modes travel essentially undistorted for shorter distances (around 20 normalized  $z$ -units, see Fig. 10) which corresponds to 24 mm. Noticeably, during propagation there was a change of 0.0133%/mm (0.245%/mm) in the soliton velocity for moderately (strongly) localized modes in which case strongly localized mode slows down and eventually relaxes to a stationary state (see Fig. 11). This behavior depends crucially on the initial amplitude. Higher amplitude solitons are less “mobile” than lower amplitude beams. The discrete Fourier transform yields a useful, but nonuniform TW solution.

#### 4. Asymptotic theory for discrete TWs

##### 4.1. Perturbation expansion around stationary solutions

We have seen in Section 3.4, that TWs with nonuniform speed can be numerically constructed by means of the Fourier iteration method. These solutions can move over short distances without drastic change in their shape or speed. However, strongly localized modes will immediately start decelerating and emitting radiation. Our conclusion from Section 3.4 was that uniform TWs for the DNLS equation are unlikely to exist. To give further support to this belief, we consider the case in which the solitons move slowly. We develop a fully discrete perturbation theory for finite amplitudes. It is important to note that our perturbative approach is fundamentally different than the perturbation methods based on inverse scattering theory (cf. [47]). We begin by taking  $\beta = \epsilon\beta_1 + O(\epsilon^2)$ ,  $\epsilon \ll 1$ , and expand the soliton velocity, frequency and the wave functions in a power series in  $\epsilon$ :

$$F = F_0 + \epsilon F_1 + \epsilon^2 F_2 + O(\epsilon^3), \quad G = \epsilon G_1 + \epsilon^2 G_2 + O(\epsilon^3), \quad (4.1)$$

$$V = \epsilon V_1 + \epsilon^2 V_2 + O(\epsilon^3), \quad \omega = \omega_s + \epsilon \omega_1 + \epsilon^2 \omega_2 + O(\epsilon^3). \quad (4.2)$$

Substituting Eqs. (4.1) and (4.2) into Eq. (3.26), we find that to leading order ( $\epsilon^0$ ),  $F_0$  satisfies the stationary equation and is even in  $\xi$ :

$$\mathcal{L}_1 F_0(\xi) = 0. \tag{4.3}$$

The order  $\epsilon$  equations for  $F_1$  and  $G_1$  are given by

$$\mathcal{L}_1 F_1 = \omega_1 F_0, \tag{4.4}$$

$$\mathcal{L}_2 G_1 = V_1 \frac{dF_0}{d\xi} + \frac{\beta_1}{h} (E_+ - E_-) F_0 \tag{4.5}$$

and the order  $\epsilon^2$  system is

$$\mathcal{L}_2 G_2 = \omega_1 G_1 + V_1 \frac{dF_1}{d\xi} + V_2 \frac{dF_0}{d\xi} - 2F_0 F_1 G_1 + \frac{\beta_1}{h} (E_+ - E_-) F_1, \tag{4.6}$$

$$\mathcal{L}_1 F_2 = \omega_1 F_1 + \omega_2 F_0 - V_1 \frac{dG_1}{d\xi} - F_0 G_1^2 - 3F_0 F_1^2 + \frac{\beta_1^2}{2} (E_+ + E_-) F_0 - \frac{\beta_1}{h} (E_+ - E_-) G_1, \tag{4.7}$$

where the linear operators  $\mathcal{L}_1$  and  $\mathcal{L}_2$  are defined by

$$\mathcal{L}_1 \mathcal{S} \equiv -\omega_s \mathcal{S} + \frac{1}{h^2} (E_+ + E_- - 2) \mathcal{S} + 3F_0^2 \mathcal{S}, \quad \mathcal{L}_2 \mathcal{S} \equiv -\omega_s \mathcal{S} + \frac{1}{h^2} (E_+ + E_- - 2) \mathcal{S} + F_0^2 \mathcal{S}. \tag{4.8}$$

Next we solve the system of equations at each order in  $\epsilon$ . By taking  $\omega_1 \partial / \partial \omega_s$  in Eq. (4.3) we find that solution to  $F_1$  is given by

$$F_1 = \omega_1 \frac{\partial F_0}{\partial \omega_s} + c_1 \frac{\partial F_0}{\partial \xi}. \tag{4.9}$$

To solve equation in (4.5), we make the ansatz:

$$G_1 = V_1 A + \beta_1 \xi F_0 + c_2 F_0, \tag{4.10}$$

where  $c_1$  and  $c_2$  are arbitrary constants and  $A$  satisfies

$$\mathcal{L}_2 A = \frac{\partial F_0}{\partial \xi}, \tag{4.11}$$

which can be solved either numerically by Fourier transform method or by reduction of order method. Note that  $A(\xi)$  is an anti-symmetric function.

#### 4.2. Solvability conditions at $O(\epsilon)$

The velocity  $V_1(\beta_1)$  and frequency shift  $\omega_1$ , are determined by a solvability condition at order  $\epsilon^2$  which is the discrete analog of Green’s identity. We start first with the order  $\epsilon$  equations. Let  $W(\xi)$  be a solution to the homogeneous equation,  $\mathcal{L}_1 W(\xi) = 0$ . Multiplying Eq. (4.4) by  $W(\xi)$  and subtracting  $F_1(\xi) \mathcal{L}_1 W(\xi) = 0$  we find

$$\Delta_\xi [Y(\xi)] = h^2 \omega_1 W(\xi) F_0(\xi), \tag{4.12}$$

where  $Y(\xi) = W(\xi - h) F_1(\xi) - F_1(\xi - h) W(\xi)$  and  $\Delta_\xi$  is defined by  $\Delta_\xi [S(\xi)] = S(\xi + h) - S(\xi)$ . An important identity which will be used frequently is the discrete analog of Green’s identity

$$\sum_{\ell=-\infty}^{+\infty} [S(\xi + \ell h) - S(\xi + (\ell - 1)h)] = 0$$

with  $\ell \in \mathbb{Z}$ . Since  $W = dF_0/d\xi$ , summing over all integers in Eq. (4.12) and using the discrete Green’s identity we find

$$\omega_1 \sum_{\ell=-\infty}^{+\infty} \left( F_0 \frac{dF_0}{d\xi} \right) \Big|_{\xi+\ell h} = 0. \tag{4.13}$$

Importantly, if  $\xi$  is not restricted to the grid points then the sum in Eq. (4.13) is generally not zero. We shall consider the case in which  $\xi \in \mathbb{Z}$  otherwise, as we will see below, no TW solution is obtained. With this assumption in mind, the solvability condition at order  $\epsilon$  is satisfied and at this stage  $\omega_1$  is an arbitrary constant. Similarly, we find that the solvability condition for Eq. (4.5) reads

$$\sum_{\ell=-\infty}^{+\infty} F_0(\xi + \ell h) \left[ V_1 \frac{dF_0}{d\xi} \Big|_{\xi+\ell h} + \frac{\beta_1}{h} (F_0(\xi + (\ell + 1)h) - F_0(\xi + (\ell - 1)h)) \right] = 0. \tag{4.14}$$

As before, if we are off the grid points then the sum in (4.14) does not necessarily vanish and as a result the velocity will depend on  $\xi$ . Therefore, we restrict the sum to the lattice points which is consistent with the discrete Fourier transform.

### 4.3. Solvability conditions at $O(\epsilon^2)$

Next we consider the solvability conditions to the  $O(\epsilon^2)$  equations which will determine the velocity  $V_1$  and frequency  $\omega_1$ . The solvability conditions for Eqs. (4.6) and (4.7), respectively, read

$$\sum_{\ell=-\infty}^{+\infty} F_0(\xi + \ell h) \left[ V_1 \frac{dF_1}{d\xi} \Big|_{\xi+\ell h} + V_2 \frac{dF_0}{d\xi} \Big|_{\xi+\ell h} + \frac{\beta_1}{h} (F_1(\xi + (\ell + 1)h) - F_1(\xi + (\ell - 1)h)) \right. \\ \left. + \omega_1 G_1(\xi + \ell h) - 2F_0(\xi + \ell h)F_1(\xi + \ell h)G_1(\xi + \ell h) \right] = 0, \tag{4.15}$$

$$\sum_{\ell=-\infty}^{+\infty} F_0(\xi + \ell h) \left[ \omega_1 F_1(\xi + \ell h) + \omega_2 F_0(\xi + \ell h) - V_1 \frac{dG_1}{d\xi} \Big|_{\xi+\ell h} - F_0(\xi + \ell h)G_1^2(\xi + \ell h) \right. \\ \left. - 3F_0(\xi + \ell h)F_1^2(\xi + \ell h) + \frac{\beta_1^2}{2} (F_0(\xi + (\ell + 1)h) + F_0(\xi + (\ell - 1)h)) \right. \\ \left. - \frac{\beta_1}{h} (G_1(\xi + (\ell + 1)h) - G_1(\xi + (\ell - 1)h)) \right] = 0. \tag{4.16}$$

Substituting the expressions for  $F_1$  and  $G_1$  [see Eqs. (4.9) and (4.10)] in Eqs. (4.15) and (4.16) and using the fact that the function  $A(\xi)$  is anti-symmetric we find

$$\begin{bmatrix} \mathbb{A}_{11} & \mathbb{A}_{12} \\ \mathbb{A}_{21} & \mathbb{A}_{22} \end{bmatrix} \begin{bmatrix} c_1 \\ c_2 \end{bmatrix} = 0, \tag{4.17}$$

where

$$\begin{aligned}
 \mathbb{A}_{11} &= V_1 \sum_{\ell=-\infty}^{+\infty} F_0(\xi + \ell h) \left[ \frac{d^2 F_0}{d\xi^2} \Big|_{\xi+\ell h} + \frac{\beta_1}{h} \left( \frac{dF_0}{d\xi} \Big|_{\xi+(\ell+1)h} - \frac{dF_0}{d\xi} \Big|_{\xi+(\ell-1)h} \right) \right] \\
 &\quad - 2V_1 \sum_{\ell=-\infty}^{+\infty} A(\xi + \ell h) F_0^2(\xi + \ell h) \frac{dF_0}{d\xi} \Big|_{\xi+\ell h} - 2\beta_1 \sum_{\ell=-\infty}^{+\infty} (\xi + \ell h) F_0^3(\xi + \ell h) \frac{dF_0}{d\xi} \Big|_{\xi+\ell h}, \\
 \mathbb{A}_{12} &= \omega_1 \sum_{\ell=-\infty}^{+\infty} F_0^2(\xi + \ell h) - 2\omega_1 \sum_{\ell=-\infty}^{+\infty} F_0^3(\xi + \ell h) \frac{dF_0}{d\omega_s}(\xi + \ell h), \\
 \mathbb{A}_{21} &= \omega_1 \sum_{\ell=-\infty}^{+\infty} \left( \frac{dF_0}{d\xi} \right)^2 \Big|_{\xi+\ell h} - 6\omega_1 \sum_{\ell=-\infty}^{+\infty} \left( \frac{dF_0}{d\xi} \right)^2 \Big|_{\xi+\ell h} F_0(\xi + \ell h) \frac{dF_0}{d\omega_s}(\xi + \ell h), \\
 \mathbb{A}_{22} &= - \sum_{\ell=-\infty}^{+\infty} \frac{dF_0}{d\xi} \Big|_{\xi+\ell h} [2\beta_1(\xi + \ell h) F_0^3(\xi + \ell h) + 2V_1 A(\xi + \ell h) F_0^2(\xi + \ell h)] \\
 &\quad - \frac{\beta_1}{h} \sum_{\ell=-\infty}^{+\infty} \frac{dF_0}{d\xi} \Big|_{\xi+\ell h} (F_0(\xi + (\ell + 1)h) - F_0(\xi + (\ell - 1)h)) - V_1 \sum_{\ell=-\infty}^{+\infty} \left( \frac{dF_0}{d\xi} \right)^2 \Big|_{\xi+\ell h}.
 \end{aligned}$$

The dependence of the velocity on  $\beta_1$  will be determined by requiring that the determinant of the matrix equation (4.17) vanish. By restricting the sum to the lattice points,  $\xi = \xi_\ell \equiv \ell h$ , which is consistent with the discrete Fourier transform we find that the results are consistent if  $\omega_1 = 0$  in which case the velocity is given by

$$\begin{aligned}
 V_1 &= -\frac{a_1}{a_2} \beta_1, \quad a_1(h) = \sum_{\ell \in \mathbb{Z}} \frac{dF_0}{d\xi} \Big|_{\xi_\ell} \left[ 2\xi_\ell F_0^3(\xi_\ell) + \frac{1}{h} (E_+ - E_-) F_0(\xi_\ell) \right], \\
 a_2(h) &= \sum_{\ell \in \mathbb{Z}} \frac{dF_0}{d\xi} \Big|_{\xi_\ell} \left[ 2A(\xi_\ell) F_0^2(\xi_\ell) + \frac{dF_0}{d\xi} \Big|_{\xi_\ell} \right].
 \end{aligned} \tag{4.18}$$

We compared these semi-analytical results with direct numerical simulation for the fully discrete case and found a good agreement for distances  $z$  of order 1. However, for longer distances, the theory needs to be modified. Moreover, in the limit  $h \rightarrow 0$  we retrieve the known result  $V_1 = -2\beta_1$ ,  $G_1(\xi) \rightarrow 0$ .

### 5. Nonlinear diffraction management

#### 5.1. Heuristic approach

Let us begin the analysis by considering an infinite array of weakly coupled optical waveguides with equal separation  $d$ . We have seen that the equation which governs the evolution of a singly polarized beam in a nonlinear waveguide array follows the discrete NLS equation. A natural generalization to two interacting electric fields  $E_n^{(1)}$  and  $E_n^{(2)}$ , is given by [13,29,30,53,54]

$$\frac{dE_n^{(j)}}{dz} = iC(E_{n+1}^{(j)} + E_{n-1}^{(j)}) + ik_w^{(j)} E_n^{(j)} + i(\mathbf{\kappa} \mathcal{E}_n)_j E_n^{(j)}, \quad j = 1, 2, \tag{5.1}$$

where  $\mathbf{\kappa}$  is a  $2 \times 2$  matrix with  $\kappa_{jj}$  and  $\kappa_{jl}$ ,  $j \neq l$  the self and cross-phase modulation coefficients, respectively, that result from the nonlinear index change,  $\mathcal{E}_n = (|E_n^{(1)}|^2, |E_n^{(2)}|^2)^T$ ,  $C$  a coupling constant,  $z$  the propagation distance

and  $k_w^{(1,2)}$  the propagation constants of the waveguides. When a cw modes of the form

$$E_n^{(1,2)}(z) = A_{1,2} \exp[i(k_z z - nk_x d)] \tag{5.2}$$

is inserted into the linearized version of Eq. (5.1) it yields

$$k_z = k_w^{(1,2)} + 2C \cos(k_x d), \quad k_z'' = -2Cd^2 \cos(k_x d), \tag{5.3}$$

where, as mentioned earlier, discrete diffraction is given by  $k_z''$ . An important consequence of Eq. (5.3) is that  $k_z''$  can have a negative sign if  $\pi/2 < |k_x d| \leq \pi$ , hence, a light beam can experience anomalous diffraction. Experimentally, the sign and local value of the diffraction can be controlled and manipulated by launching light at a particular angle with respect to the normal to the waveguides or equivalently by tilting the waveguide array. To build a nonlinear model of diffraction management, we use a cascade of different segments of the waveguide, each piece being tilted by an angle zero and  $\gamma_w$ , respectively. The actual physical angle  $\gamma_w$  (the waveguide tilt angle) is related to the wavenumber  $k_x$  by the relation [27]  $\sin \gamma_w = k_x/k$  where  $k = 2\pi n_0/\lambda_0$  ( $\lambda_0 = 1.53 \mu\text{m}$  is the central wavelength in vacuum and we take  $n_0 = 3.3$  to be the linear refractive index). In this way, we generate a waveguide array with alternating diffraction. Next, we define the dimensionless amplitudes  $U_n^{(j)}$  ( $U_n^{(1)} \equiv U_n, U_n^{(2)} \equiv V_n$ ) by

$$E_n^{(j)} = \sqrt{P_*} U_n^{(j)} e^{i(k_w^{(j)} + 2C)z}, \quad z' = \frac{z}{z_*}, \tag{5.4}$$

where  $P_* = \max(|U_n|_{\max}^2, |V_n|_{\max}^2)$  is the characteristic power and  $z_*$  the nonlinear length scale. Substituting these quantities into Eq. (5.1) yields the following (dropping the prime) diffraction-managed vector DNLS equations [29,30]:

$$\begin{aligned} i \frac{dU_n}{dz} + \frac{D(z/z_w)}{2h^2} (U_{n+1} + U_{n-1} - 2U_n) + (|U_n|^2 + \eta|V_n|^2)U_n &= 0, \\ i \frac{dV_n}{dz} + \frac{D(z/z_w)}{2h^2} (V_{n+1} + V_{n-1} - 2V_n) + (\eta|U_n|^2 + |V_n|^2)V_n &= 0, \end{aligned} \tag{5.5}$$

where  $\eta = \kappa_{12}/\kappa_{11}$  (we take  $\kappa_{11} = \kappa_{22}, \kappa_{12} = \kappa_{21}$ ) and  $z_* = 1/(\kappa_{11} P_*)$ . We choose  $z_* C \cos(k_x d) = D(z/z_w)/(2h^2)$  where  $D(z/z_w)$  is a piecewise constant periodic function that measures the local value of diffraction. Here  $z_w \equiv 2L/z_*$  with  $L$  being the physical length of each waveguide segment (see Fig. 12(a) for schematic representation). Eq. (5.5) describe the dynamical evolution of coupled beams in a Kerr medium with varying diffraction. When the “effective” nonlinearity balances the average diffraction then bright vector discrete solitons can form. The dependence of the coupling constant  $C$  on the waveguide width ( $\ell$ ) and separation ( $d$ ) is given by (for AlGaAs waveguide)  $C = (0.00984/\ell) \exp(-0.22d)$  (see Eq. 13.8-10, pp. 523 of Ref. [55]). Therefore, the coupling constant  $C$  that corresponds to the experimental data reported in [28] (for  $2.5 \mu\text{m}$  waveguide separation and width) is found

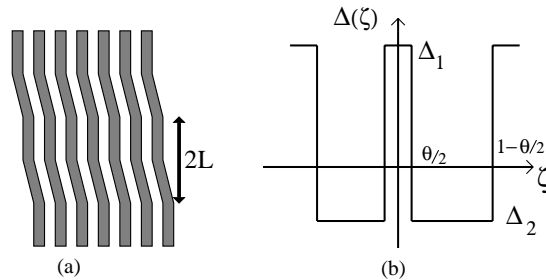


Fig. 12. Schematic presentation of the waveguide array (a) and the diffraction map (b).

to be  $C = 2.27 \text{ mm}^{-1}$ . For typical power  $P_* \approx 300 \text{ W}$ ; typical nonlinear Kerr coefficient  $\kappa_{11} = 3.6 \text{ m}^{-1} \text{ W}^{-1}$  and typical waveguide length  $L \approx 100 \mu\text{m}$  we find  $z_* \approx 1 \text{ mm}$  and  $z_w \approx 0.2$ , which suggests the use of asymptotic theory based on small  $z_w$ . Such asymptotic analysis was developed in [29,30] for both the scalar and vector cases where the diffraction function  $D = \delta_1 + \Delta/z_w$  with  $\Delta$  being a piecewise constant function (see Fig. 12(b)). Model (5.5) admits stationary soliton solution even when  $z_w$  is of order 1.

## 5.2. Asymptotic theory for diffraction management

### 5.2.1. Renormalization

We have seen in the preceding section how can we build, based on physical heuristic arguments, a model that incorporate both normal and anomalous diffraction. The key idea in formulating a model of diffraction management, is to use a cascade of different segments of waveguide, each piece being tilted by an angle zero and  $\gamma$ , respectively. Here, we give a derivation of the model, in the scalar case, based on asymptotic theory. Two approaches are given. The first is based on perturbation expansion using a renormalized eigen-mode of each single waveguide, whereas in the second we expand around eigenfunction of an untilted waveguide. It is clear from Fig. 12(a) that each single waveguide is not stationary. As a result, the evolution of the beam’s amplitude is governed by

$$\left(\frac{\partial^2}{\partial z^2} + \frac{\partial^2}{\partial x^2}\right)\Psi + k_0^2 f^2(X)\Psi = 0, \quad X = x - \frac{\alpha}{\varepsilon} \int_0^Z D(Z') dZ', \tag{5.6}$$

whereas before,  $Z = \varepsilon z$ ;  $\alpha$  is a small parameter to be determined later and  $D(Z)$  a *piecewise constant* periodic function that measures the local value of diffraction. When the waveguides are well separated then the dynamics of each mode  $\psi_m$  in waveguide  $f_m^2$  is decoupled and is given by

$$(\alpha^2 D^2(Z) + 1) \frac{d^2 \psi_m}{dX^2} + (k_0^2 f_m^2(X) - \lambda_0^2) \psi_m = 0. \tag{5.7}$$

However when the waveguides are at close proximity, we approximate the solution to Eq. (5.6) as a multiscale perturbation series:

$$\Psi = \sum_{m=-\infty}^{+\infty} E_m(Z) \psi_m(X) e^{-i\lambda_0 z}. \tag{5.8}$$

Substituting the ansatz (5.8) into Eq. (5.6), we find

$$\sum_{m=-\infty}^{+\infty} \left[ -2i\varepsilon\lambda_0 \psi_m \frac{\partial E_m}{\partial Z} + \varepsilon^2 \psi_m \frac{\partial^2 E_m}{\partial Z^2} + \left( (\alpha^2 D^2 + 1) \frac{d^2 \psi_m}{dX^2} + k_0^2 f^2 \psi_m - \lambda_0^2 \psi_m \right) E_m + 2i\alpha\lambda_0 D E_m \frac{d\psi_m}{dX} - 2\alpha\varepsilon D \frac{\partial E_m}{\partial Z} \frac{d\psi_m}{dX} - \alpha\varepsilon E_m \frac{dD}{dZ} \frac{d\psi_m}{dX} \right] e^{-i\lambda_0 z} = 0. \tag{5.9}$$

Using Eq. (5.7) in the above equation, multiplying Eq. (5.9) by  $\psi_n^* \exp(i\lambda_0 z)$  and integrating over  $X$  yields the following:

$$\sum_{m=-\infty}^{+\infty} \left[ \left( -2i\varepsilon\lambda_0 \frac{\partial E_m}{\partial Z} + \varepsilon^2 \frac{\partial^2 E_m}{\partial Z^2} \right) \int_{-\infty}^{+\infty} dX \psi_m \psi_n^* + k_0^2 E_m \int_{-\infty}^{+\infty} dX \Delta f_m^2 \psi_m \psi_n^* + 2i\alpha\lambda_0 D E_m \int_{-\infty}^{+\infty} dX \frac{d\psi_m}{dX} \psi_n^* - \varepsilon\alpha \left( 2D \frac{\partial E_m}{\partial Z} + E_m \frac{dD}{dZ} \right) \int_{-\infty}^{+\infty} dX \frac{d\psi_m}{dX} \psi_n^* \right] = 0. \tag{5.10}$$

Similar to the arguments we presented before, we shall assume that the overlap integrals follow the scaling given in Eq. (2.6) and that  $\alpha = O(\mu)$ . In close analogy to the calculations given before, we find that for a sech-like mode (Eq. (2.7)) profile we have

$$\int_{-\infty}^{+\infty} dX \frac{d\psi_m}{dX} \psi_n^* = \frac{b}{\mu} e^{-|n-m|/\mu}, \quad (5.11)$$

where  $b$  is a constant. Restricting the sum in Eq. (5.10) to the nearest neighbors, i.e.,  $m = n, n \pm 1$  and by defining  $\tilde{z} = Z/(2\lambda_c a_0)$ ,  $k_0^2 c_1 = C_1$ ,  $2\lambda_c bD = \tilde{D}$ ;  $E_n = \tilde{E}_n \exp(-ik_0^2 c_0 \tilde{z})$  we find that  $E_n$  satisfies (dropping the tilde)

$$i \frac{\partial E_n}{\partial z} + C_1(E_{n+1} + E_{n-1}) + iD(z)(E_{n+1} - E_{n-1}) = 0. \quad (5.12)$$

The constant diffraction case, i.e., Eq. (2.10) is recovered when  $D = 0$ . Eq. (5.12) is the general dynamical equation that governs the evolution of optical beam in a diffraction-managed linear waveguide array. However, when the intensity of the incident beam is sufficiently high then the refractive index of the medium will depend on the intensity which for Kerr media is proportional to the intensity. Therefore, by following the same procedure outlined in Section 2.1 we find that the general evolution equation for the optical field in a diffraction-managed nonlinear waveguide array is governed by

$$i \frac{\partial E_n}{\partial z} + C_1(E_{n+1} + E_{n-1}) + iD(z)(E_{n+1} - E_{n-1}) + g_{nl}|E_n|^2 E_n = 0. \quad (5.12)$$

In the case of strong diffraction for which  $\max |D(z)| \gg |C_1|$  (recall that  $D(z)$  is a piecewise constant function) and by defining  $E_n = E_n \exp(-i\pi n/2)$ , Eq. (5.12) reduces to

$$i \frac{\partial E_n}{\partial z} + D(z)(E_{n+1} + E_{n-1}) + g_{nl}|E_n|^2 E_n = 0. \quad (5.13)$$

### 5.2.2. Direct approach

In this section, we give a different approach to derive a model for diffraction management. We approximate the solution to Eq. (5.6) again as a multiscale perturbation series:

$$\Psi = \sum_{m=-\infty}^{+\infty} E_m(Z) \psi_m(X) e^{i[\varphi_m(z) - \lambda_0 z]}, \quad (5.14)$$

where the the phase  $\varphi_m(z)$  will be chosen later. Substituting the ansatz (5.14) into Eq. (5.6), we find

$$\sum_{m=-\infty}^{+\infty} e^{i[\varphi_m(z) - \lambda_0 z]} \left[ E_m \frac{d^2 \psi_m}{dX^2} (1 + \alpha^2 D^2) + k_0^2 f^2 E_m \psi_m + 2i \left( \frac{d\varphi_m}{dz} - \lambda_0 \right) \left( \varepsilon \frac{\partial E_m}{\partial Z} \psi_m - \alpha D \frac{d\psi_m}{dX} E_m \right) \right. \\ \left. - \left( \frac{d\varphi_m}{dz} - \lambda_0 \right)^2 E_m \psi_m - 2\alpha \varepsilon D \frac{\partial E_m}{\partial Z} \frac{d\psi_m}{dX} - \alpha \varepsilon E_m \frac{dD}{dZ} \frac{d\psi_m}{dX} + i \frac{d^2 \varphi_m}{dz^2} E_m \psi_m + \varepsilon^2 \frac{\partial E_m}{\partial Z} \psi_m \right] = 0. \quad (5.15)$$

Using Eq. (2.1) and multiplying Eq. (5.15) by  $\psi_n^* \exp[-i\varphi_n(z)]$  and integrating over  $-\infty < X < \infty$  yields the following equation (ignoring the order  $\varepsilon^2$  term):

$$\sum_{m=-\infty}^{+\infty} e^{i[\varphi_m(z)-\varphi_n(z)]} \left\{ \mathbf{E}_m \int dX \psi_m \psi_n^* \left[ \alpha^2 \mathbf{D}^2 (\lambda_0^2 - k_0^2 f_m^2) + k_0^2 \Delta f_m^2 - \left( \frac{d\varphi_m}{dz} \right)^2 + 2\lambda_0 \frac{d\varphi_m}{dz} + i \frac{d^2 \varphi_m}{dz^2} \right] \right. \\ \left. - \alpha \left[ \mathbf{E}_m \left( 2i \left( \frac{d\varphi_m}{dz} - \lambda_0 \right) \mathbf{D} + \frac{d\mathbf{D}}{dZ} \right) + 2\varepsilon \mathbf{D} \frac{\partial \mathbf{E}_m}{\partial Z} \right] \right. \\ \left. \times \int dX \frac{d\psi_m}{dX} \psi_n^* + 2i\varepsilon \left( \frac{d\varphi_m}{dz} - \lambda_0 \right) \frac{\partial \mathbf{E}_m}{\partial Z} \int dX \psi_m \psi_n^* \right\} = 0.$$

Until now the phase factor  $\varphi_m$  is arbitrary. Therefore, we shall choose the phase in such a way that

$$\alpha^2 \mathbf{D}^2 \int_{-\infty}^{+\infty} dX (\lambda_0^2 - k_0^2 f_m^2) |\psi_m|^2 = \left[ \left( \frac{d\varphi_m}{dz} \right)^2 - 2\lambda_0 \frac{d\varphi_m}{dz} \right] \int_{-\infty}^{+\infty} dX |\psi_m|^2. \tag{5.16}$$

Eq. (5.16) implies that

$$\frac{d\varphi_m}{dz} = O(\alpha^2), \quad \left( \frac{d\varphi_m}{dz} \right)^2 = O(\alpha^4), \quad \frac{d^2 \varphi_m}{dz^2} = O(\alpha \varepsilon). \tag{5.17}$$

The localized nature of the waveguides indicates that  $\varphi_m$  is independent of  $m$ , i.e., it is the same for all waveguides. With this scaling in mind and by taking as before  $\alpha = O(\mu)$ , we recover Eq. (5.12).

### 5.3. Asymptotic theory for vector diffraction management

In this section we present a derivation of the vector DM-DNLS equation starting from the nonlinear vector Helmholtz equations which is obtained from Maxwell’s equations. The propagation of an intense laser beam in a Kerr medium is described by the vector Helmholtz equations:

$$\left( \frac{\partial^2}{\partial x^2} + \frac{\partial^2}{\partial z^2} \right) \mathbf{E} + \delta \nabla (\nabla \cdot \mathbf{P}_{NL}) + k_0^2 f^2(x) \mathbf{E} + \delta \mathbf{P}_{NL} = 0. \tag{5.18}$$

The nonlinear polarization  $\mathbf{P}_{NL}$  can be expressed in terms of the electric field as

$$\mathbf{P}_{NL} = (\mathbf{E} \cdot \mathbf{E}^*) \mathbf{E} + \gamma (\mathbf{E} \cdot \mathbf{E}) \mathbf{E}^*, \tag{5.19}$$

where  $\gamma$  is a constant related to the third order nonlinear susceptibility [56]. Since we are interested in interaction between two coupled laser beams, we shall assume that each one is initially linearly polarized and mutually orthogonal, i.e.:

$$\mathbf{E}(x, z) = \mathcal{E}_1(x, z) \hat{\mathbf{x}} + \mathcal{E}_2(x, z) \hat{\mathbf{y}} + \mathcal{E}_3(x, z) \hat{\mathbf{z}}. \tag{5.20}$$

In this case, the nonlinear polarization takes the form

$$\mathbf{P}_{NL} = P_{NL}^{(1)} \hat{\mathbf{x}} + P_{NL}^{(2)} \hat{\mathbf{y}} + P_{NL}^{(3)} \hat{\mathbf{z}}, \tag{5.21}$$

where

$$P_{NL}^{(1)} = ((1 + \gamma) |\mathcal{E}_1|^2 + |\mathcal{E}_2|^2) \mathcal{E}_1 + \gamma \mathcal{E}_2^2 \mathcal{E}_1^* + \gamma \mathcal{E}_3^2 \mathcal{E}_1^*, \tag{5.22}$$

$$P_{NL}^{(2)} = (|\mathcal{E}_1|^2 + (1 + \gamma) |\mathcal{E}_2|^2) \mathcal{E}_2 + \gamma \mathcal{E}_1^2 \mathcal{E}_2^* + \gamma \mathcal{E}_3^2 \mathcal{E}_2^*, \tag{5.23}$$

$$P_{NL}^{(3)} = (|\mathcal{E}_1|^2 + |\mathcal{E}_2|^2 + (1 + \gamma) |\mathcal{E}_3|^2) \mathcal{E}_3 + \gamma \mathcal{E}_1^2 \mathcal{E}_3^* + \gamma \mathcal{E}_2^2 \mathcal{E}_3^*. \tag{5.24}$$

Substituting the expression for  $\mathbf{E}$  in Eq. (5.18) and taking into account the nonlinear polarization, leads to the coupled system:

$$\left(\frac{\partial^2}{\partial x^2} + \frac{\partial^2}{\partial z^2}\right) \mathcal{E}_1 + \delta \frac{\partial^2 P_{\text{NL}}^{(1)}}{\partial x^2} + k_0^2 f^2(x) \mathcal{E}_1 + \delta P_{\text{NL}}^{(1)} = 0, \quad (5.25)$$

$$\left(\frac{\partial^2}{\partial x^2} + \frac{\partial^2}{\partial z^2}\right) \mathcal{E}_2 + k_0^2 f^2(x) \mathcal{E}_2 + \delta P_{\text{NL}}^{(2)} = 0, \quad (5.26)$$

$$\left(\frac{\partial^2}{\partial x^2} + \frac{\partial^2}{\partial z^2}\right) \mathcal{E}_3 + \delta \frac{\partial^2 P_{\text{NL}}^{(1)}}{\partial x \partial z} + \delta \frac{\partial^2 P_{\text{NL}}^{(3)}}{\partial z^2} + k_0^2 f^2(x) \mathcal{E}_3 + \delta P_{\text{NL}}^{(3)} = 0. \quad (5.27)$$

In this work, we are interested in interaction of two mutually orthogonal beams. However, if we initially assume that  $\mathcal{E}_3 = 0$ , then the source term  $\partial^2 P_{\text{NL}}^{(1)}/\partial x \partial z$  appearing in Eq. (5.27) will eventually generate a nonzero  $\mathcal{E}_3$  component. In fact, this additional term (due to nonlinear polarization) is of order  $\delta$ . Hence, we are justified in neglecting  $\mathcal{E}_3$  as compared to  $\mathcal{E}_1$  and  $\mathcal{E}_2$ . Next we follow the same expansion as mentioned earlier and let

$$\mathcal{E}_1 = \sum_{m=-\infty}^{+\infty} A_m(Z) \psi_m(X) e^{-i\lambda_0 z}, \quad \mathcal{E}_2 = \sum_{m=-\infty}^{+\infty} B_m(Z) \psi_m(X) e^{-i\lambda_0 z}, \quad (5.28)$$

where  $X$  has been defined in Eq. (5.6). The expansion of the linear terms is already given in (5.12) with the addition of on-site terms  $k_{\text{wg}} A_n$  and  $k_{\text{wg}} B_n$ . Therefore, we focus the attention below solely on the nonlinear terms and in particular give an estimate on the order of magnitude of  $\partial^2 P_{\text{NL}}^{(1)}/\partial x^2$ . Substituting the ansatz (5.28) into Eqs. (5.25) and (5.26); multiplying by  $\psi_n^* \exp(i\lambda_0 z)$  and integrating over  $X$  yields the following result for the nonlinear terms:

$$\begin{aligned} \int_{-\infty}^{+\infty} dX P_{\text{NL}}^{(1)} \psi_n^* e^{i\lambda_0 z} &= (1 + \gamma) \sum_{m, m', m''} A_m A_{m'} A_{m''}^* \int_{-\infty}^{+\infty} dX \psi_m \psi_{m'} \psi_{m''}^* \psi_n^* \\ &+ \sum_{j, j', j''} B_j B_{j'}^* A_{j''} \int_{-\infty}^{+\infty} dX \psi_j \psi_{j'} \psi_{j''}^* \psi_n^* + \gamma \sum_{l, l', l''} B_l B_{l'} A_{l''}^* \int_{-\infty}^{+\infty} dX \psi_l \psi_{l'} \psi_{l''}^* \psi_n^*. \end{aligned} \quad (5.29)$$

$$\begin{aligned} \int_{-\infty}^{+\infty} dX P_{\text{NL}}^{(2)} \psi_n^* e^{i\lambda_0 z} &= \sum_{m, m', m''} A_m A_{m'}^* B_{m''} \int_{-\infty}^{+\infty} dX \psi_m \psi_{m'} \psi_{m''}^* \psi_n^* + (1 + \gamma) \sum_{j, j', j''} B_j B_{j'} B_{j''}^* \\ &\times \int_{-\infty}^{+\infty} dX \psi_j \psi_{j'} \psi_{j''}^* \psi_n^* + \gamma \sum_{l, l', l''} A_l A_{l'} B_{l''}^* \int_{-\infty}^{+\infty} dX \psi_l \psi_{l'} \psi_{l''}^* \psi_n^*. \end{aligned} \quad (5.30)$$

Due to the assumption of widely separated waveguides, the only order 1 contribution comes from the nonlinear term when  $m = m' = m'' = n$ . We therefore find that to  $O(\varepsilon)$  the nonlinear evolution of  $A_n$  and  $B_n$  is given by (taking  $\delta = \varepsilon$ )

$$i \frac{\partial A_n}{\partial z} + k_{\text{wg}} A_n + \mathcal{C}(z) A_{n+1} + \mathcal{C}^*(z) A_{n-1} + (\tilde{a}_1 |A_n|^2 + \tilde{b}_1 |B_n|^2) A_n + \tilde{\eta}_1 B_n^2 A_n^* = 0, \quad (5.31)$$

$$i \frac{\partial B_n}{\partial z} + k_{\text{wg}} B_n + \mathcal{C}(z) B_{n+1} + \mathcal{C}^*(z) B_{n-1} + (\tilde{a}_2 |B_n|^2 + \tilde{b}_2 |A_n|^2) B_n + \tilde{\eta}_2 A_n^2 B_n^* = 0, \quad (5.32)$$

where the coefficients  $\tilde{a}_1, \tilde{a}_2, \tilde{b}_1, \tilde{b}_2, \tilde{\eta}_1, \tilde{\eta}_2$  are given by

$$\tilde{a}_1 = (1 + \gamma) \eta_{\text{nl}} + \gamma_{\text{nl}}, \quad \tilde{b}_1 = \eta_{\text{nl}} + \gamma_{\text{nl}}, \quad \tilde{a}_2 = (1 + \gamma) \eta_{\text{nl}}, \quad \tilde{b}_2 = \eta_{\text{nl}}, \quad \tilde{\eta}_1 = \gamma \eta_{\text{nl}} + \gamma_{\text{nl}}, \quad \tilde{\eta}_2 = \gamma \eta_{\text{nl}},$$

and

$$\int_{-\infty}^{+\infty} dX |\psi_n|^4 = \eta_{n1}, \quad \int_{-\infty}^{+\infty} dX \frac{\partial^2}{\partial X^2} (|\psi_n|^2 \psi_n) \psi_n^* = \gamma_{n1}.$$

By rescaling the field amplitudes, i.e.,  $A_n = \tilde{A}_n/\sqrt{\tilde{a}_1}$ ,  $B_n = \tilde{B}_n/\sqrt{\tilde{a}_2}$  we find the system (dropping the tilde):

$$\begin{aligned} i \frac{\partial A_n}{\partial z} + k_{\text{wg}} A_n + C(z) A_{n+1} + C^*(z) A_{n-1} + (|A_n|^2 + b_1 |B_n|^2) A_n + \eta_1 B_n^2 A_n^* &= 0, \\ i \frac{\partial B_n}{\partial z} + k_{\text{wg}} B_n + C(z) B_{n+1} + C^*(z) B_{n-1} + (|B_n|^2 + b_2 |A_n|^2) B_n + \eta_2 A_n^2 B_n^* &= 0, \end{aligned}$$

with  $b_1 = \tilde{b}_1/\tilde{a}_2$ ,  $b_2 = \tilde{b}_2/\tilde{a}_1$ ,  $\eta_1 = \tilde{\eta}_1/\tilde{a}_2$ ,  $\eta_2 = \tilde{\eta}_2/\tilde{a}_1$  (see also Section 1).

## 6. Conclusions

Localized, stable nonlinear waves, often referred to as solitons, are of broad interest in mathematics and physics. They are found in both continuous and discrete media. In this paper, a unified method is presented which is used to obtain soliton solutions to discrete problems. In recent experiments, discrete solitons were observed in an optical waveguide array. The fundamental governing system is the scalar DNLS equation. A suitable modification of this system describes diffraction-managed solitons.

In this paper we have derived and investigated scalar and vector discrete diffraction-managed systems. The proposed vector model describes propagation of two polarization modes interacting in a waveguide array with Kerr nonlinearity in the presence of varying diffraction. The coupling of the two fields is described via a cross-phase modulation coefficient. In the regime of normal diffraction, both stationary and moving discrete solitons are analyzed using the Fourier transform method. The results indicate that a continuous stationary solution and a TW solutions with uniform velocity are unlikely to exist. In the presence of both normal and anomalous diffraction a model is developed from first principles that governs the propagation of two polarization modes interacting in a nonlinear waveguide array via cross-phase modulation coupling.

## Acknowledgements

MJA is partially supported by the Air Force Office of Scientific Research, under grant number F49620-00-1-0031, and NSF under grant number DMS-0070792.

## References

- [1] E. Fermi, J. Pasta, S. Ulam, Studies of nonlinear problems, Los Alamos Report LA1940, 1955.
- [2] O.M. Braun, Y.S. Kivshar, Nonlinear dynamics of the Frenkel–Kontorova model, *Phys. Rep.* 306 (1998) 1–108.
- [3] D. Henning, G.P. Tsironis, Wave transmission in nonlinear lattices, *Phys. Rep.* 307 (1999) 333–432.
- [4] S. Flach, C.R. Willis, Discrete breathers, *Phys. Rep.* 295 (1998) 181–264.
- [5] F. Lederer, J.S. Aitchison, Discrete solitons in nonlinear waveguide arrays, in: V.E. Zakharov, S. Wabnitz (Eds.), *Les Houches Workshop on Optical Solitons*, Springer, Berlin, 1999, pp. 349–365.
- [6] A.C. Scott, L. Macneil, Binding-energy versus nonlinearity for a small stationary soliton, *Phys. Lett. A* 98 (1983) 87–88.
- [7] A.J. Sievers, S. Takeno, Intrinsic localized modes in anharmonic crystals, *Phys. Rev. Lett.* 61 (1988) 970–973.
- [8] W.P. Su, J.R. Schieffer, A.J. Heeger, Solitons in polyacetylene, *Phys. Rev. Lett.* 42 (1979) 698–1701.
- [9] A.S. Davydov, Theory of contraction of proteins under their excitation, *J. Theor. Biol.* 38 (1973) 559–569.

- [10] P. Marquii, J.M. Bilbaut, M. Remoissenet, Observation of nonlinear localized modes in an electrical lattice, *Phys. Rev. E* 51 (1995) 6127–6133.
- [11] H. Eisenberg, Y. Silberberg, R. Morandotti, in: A. Boyd, J. Aitchison (Eds.), *Discrete Spatial Optical Solitons in Waveguide Arrays*, *Phys. Rev. Lett.* 81 (1998) 3383–3386.
- [12] R. Morandotti, U. Peschel, J. Aitchison, H. Eisenberg, Y. Silberberg, Dynamics of discrete solitons in optical waveguide array, *Phys. Rev. Lett.* 83 (1999) 2726–2729.
- [13] D.N. Christodoulides, R.J. Joseph, Discrete self-focusing in nonlinear arrays of coupled wave-guides, *Opt. Lett.* 13 (1988) 794–796.
- [14] Y.S. Kivshar, Self-localization in arrays of defocusing waveguides, *Opt. Lett.* 18 (1993) 1147–1149.
- [15] W. Krolikowski, Y.S. Kivshar, Soliton-based optical switching in waveguide arrays, *J. Opt. Soc. Am. B* 13 (1996) 876–887.
- [16] A.B. Aceves, C. De Angelis, S. Trillo, S. Wabnitz, Storage and steering of self-trapped discrete solitons in nonlinear wave-guide arrays, *Opt. Lett.* 19 (1994) 332–334.
- [17] B. Malomed, M.I. Weinsrein, Soliton dynamics in the discrete nonlinear Schrödinger equations, *Phys. Lett. A* 220 (1996) 91–96.
- [18] A.B. Aceves, C. De Angelis, T. Peschel, R. Muschall, F. Lederer, S. Trillo, S. Wabnitz, Discrete self-trapping, soliton interactions, and beam steering in nonlinear waveguide arrays, *Phys. Rev. E* 53 (1996) 1172–1189.
- [19] A.B. Aceves, C. De Angelis, A.M. Rubenchik, S.K. Turitsyn, Multidimensional solitons in fiber arrays, *Opt. Lett.* 19 (1994) 329–331.
- [20] F. Lederer, S. Darmanyany, A. Kobayakov, Discrete solitons, in: S. Trillo, W. Torruellas (Eds.), *Spatial Solitons*, Springer, Berlin, 2001, pp. 267–290.
- [21] P.G. Kevrekidis, K.Ø. Rasmussen, A.R. Bishop, The discrete nonlinear Schrödinger equation: a survey of recent results, *Int. J. Mod. Phys. B* 15 (2001) 2833–2900.
- [22] T. Peschel, U. Peschel, F. Lederer, Discrete bright solitary waves in quadratically nonlinear media, *Phys. Rev. E* 57 (1998) 1127–1133.
- [23] S. Darmanyany, A. Kobayakov, F. Lederer, Strongly localized modes in discrete systems with quadratic nonlinearity, *Phys. Rev. E* 57 (1998) 2344–2349.
- [24] R. Morandotti, U. Peschel, J. Aitchison, H. Eisenberg, in: Y. Silberberg (Ed.), *Experimental Observation of Linear and Nonlinear Optical Bloch Oscillations*, *Phys. Rev. Lett.* 83 (1999) 4756–4759.
- [25] T. Pertsch, P. Dannberg, W. Elflein, A. Bräuer, F. Lederer, Optical bloch oscillations in temperature tuned waveguide arrays, *Phys. Rev. Lett.* 83 (1999) 4752–4755.
- [26] G. Lenz, I. Talanina, C. Martijn de Sterke, Bloch oscillations in an array of curved optical waveguides, *Phys. Rev. Lett.* 83 (1999) 963–966.
- [27] H. Eisenberg, Y. Silberberg, R. Morandotti, J. Aitchison, Diffraction management, *Phys. Rev. Lett.* 85 (2000) 1863–1866.
- [28] R. Morandotti, H. Eisenberg, Y. Silberberg, M. Sorel, J. Aitchison, Self-focusing and defocusing in waveguide arrays, *Phys. Rev. Lett.* 86 (2001) 3296–3299.
- [29] M.J. Ablowitz, Z.H. Musslimani, Discrete diffraction managed spatial solitons, *Phys. Rev. Lett.* 87 (2001) 254102.
- [30] M.J. Ablowitz, Z.H. Musslimani, Discrete vector spatial solitons in a nonlinear waveguide array, *Phys. Rev. E* 65 (2002) 056618.
- [31] S.F. Mingaleev, Y.S. Kivshar, Self-trapping and stable localized modes in nonlinear photonic crystals, *Phys. Rev. Lett.* 86 (2001) 5474–5477.
- [32] A.A. Sukhorukov, Y.S. Kivshar, Nonlinear localized waves in a periodic medium, *Phys. Rev. Lett.* 87 (2001) 083901.
- [33] A.A. Sukhorukov, Y.S. Kivshar, Spatial optical solitons in nonlinear photonic crystals, *Phys. Rev. E* 65 (2002) 036609.
- [34] A. Trombettoni, A. Smerzi, Discrete solitons and breathers with dilute Bose–Einstein condensates, *Phys. Rev. Lett.* 86 (2001) 2353–2356.
- [35] D.N. Christodoulides, E.D. Eugenieva, Blocking and routing discrete solitons in two-dimensional networks of nonlinear waveguide arrays, *Phys. Rev. Lett.* 87 (2001) 233901.
- [36] D.N. Christodoulides, E.D. Eugenieva, Minimizing bending losses in two-dimensional discrete soliton networks, *Opt. Lett.* 26 (2001) 1876–1878.
- [37] E.D. Eugenieva, N.K. Efremidis, D.N. Christodoulides, Design of switching junctions for two-dimensional discrete soliton, *Opt. Lett.* 26 (2001) 1978–1980.
- [38] E.D. Eugenieva, N.K. Efremidis, D.N. Christodoulides, *Opt. Photonics News* 12 (2001) 57.
- [39] D.N. Christodoulides, N.K. Efremidis, Discrete temporal solitons along a chain of nonlinear coupled microcavities embedded in photonic crystals, *Opt. Lett.* 27 (2002) 568–570.
- [40] M.J. Ablowitz, J.F. Ladik, Nonlinear differential-difference equations and Fourier-analysis, *J. Math. Phys.* 17 (1976) 1011–1018.
- [41] M. Peyrard, M.D. Kruskal, Kink dynamics in the highly discrete sine-Gordon system, *Physica D* 14 (1984) 88–102.
- [42] V.I. Petviashvili, Equation of an extraordinary soliton, *Sov. J. Plasma Phys.* 2 (257) (1976).
- [43] M.J. Ablowitz, G. Biondini, Multiscale pulse dynamics in communication systems with strong dispersion management, *Opt. Lett.* 23 (1998) 1668–1670.
- [44] S. Flach, K. Kladko, Moving discrete breathers?, *Physica D* 127 (1999) 61–72.
- [45] S. Flach, Y. Zolotaryuk, K. Kladko, Moving lattice kinks and pulses: an inverse method, *Phys. Rev. E* 59 (1999) 6105–6115.
- [46] S. Aubry, T. Cretegny, Mobility and reactivity of discrete breathers, *Physica D* 119 (1998) 34–46.
- [47] Ch. Claude, Y.S. Kivshar, O. Kluth, K.H. Spatschek, Moving localized modes in nonlinear lattices, *Phys. Rev. B* 47 (1993) 14228–14232.
- [48] M.J. Ablowitz, Z.H. Musslimani, G. Biondini, Methods for discrete solitons in nonlinear lattices, *Phys. Rev. E* 65 (2002) 026602.
- [49] V.I. Karpman, Evolution of solitons described by higher-order nonlinear Schrödinger equations, *Phys. Lett. A* 244 (1998) 397–400.
- [50] M. Karlsson, A. Höök, Soliton-like pulses governed by fourth order dispersion in optical fibers, *Opt. Commun.* 104 (1994) 303–307.
- [51] H. Feddersen, *Lecture Notes in Physics*, Springer, Berlin, 1991, pp. 159–167.

- [52] D.B. Duncan, J.C. Eilbeck, H. Feddersen, J.A.D. Wattis, Solitons on lattices, *Physica D* 68 (1993) 1–11.
- [53] S. Darmanyanyan, A. Kobayakov, E. Schmidt, F. Lederer, Strongly localized vectorial modes in nonlinear waveguide arrays, *Phys. Rev. E* 57 (1998) 3520–3530.
- [54] S. Somekh, E. Garmire, A. Yariv, H.L. Garvin, R.G. Hunsperger, Channel optical waveguide directional couplers, *Appl. Phys. Lett.* 22 (1973) 46–47.
- [55] A. Yariv, *Optical Electronics*, 5th ed., Oxford University Press, Oxford, 1997.
- [56] R.W. Boyd, *Nonlinear Optics*, Wiley, New York, 1992.